

ARMY RESEARCH LABORATORY



# Investigation of Surface Intergranular Attack and Its Effects on the Fatigue Properties of AM355 Stainless Steel

Scott Grendahl  
Victor Champagne

ARL-TR-1238

November 1996

DTIC QUALITY INSPECTED 4

19961223 098

## **NOTICES**

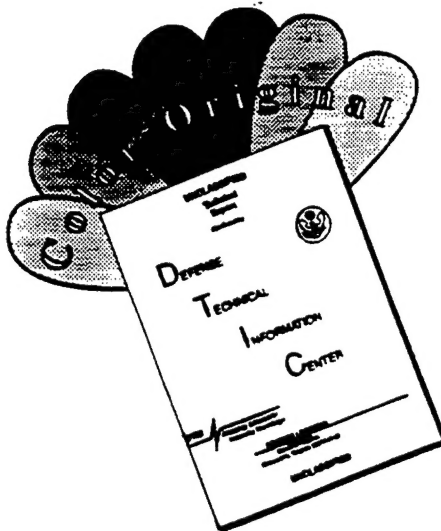
Destroy this report when it is no longer needed. DO NOT return it to the originator.

Additional copies of this report may be obtained from the National Technical Information Service, U.S. Department of Commerce, 5285 Port Royal Road, Springfield, VA 22161.

The findings of this report are not to be construed as an official Department of the Army position, unless so designated by other authorized documents.

The use of trade names or manufacturers' names in this report does not constitute indorsement of any commercial product.

# **DISCLAIMER NOTICE**



**THIS DOCUMENT IS BEST  
QUALITY AVAILABLE. THE COPY  
FURNISHED TO DTIC CONTAINED  
A SIGNIFICANT NUMBER OF  
COLOR PAGES WHICH DO NOT  
REPRODUCE LEGIBLY ON BLACK  
AND WHITE MICROFICHE.**

# REPORT DOCUMENTATION PAGE

*Form Approved  
OMB No. 0704-0188*

Public reporting burden for this collection of information is estimated to average 1 hour per response, including the time for reviewing instructions, searching existing data sources, gathering and maintaining the data needed, and completing and reviewing the collection of information. Send comments regarding this burden estimate or any other aspect of this collection of information, including suggestions for reducing this burden, to Washington Headquarters Services, Directorate for Information Operations and Reports, 1215 Jefferson Davis Highway, Suite 1204, Arlington, VA 22202-4302, and to the Office of Management and Budget, Paperwork Reduction Project(0704-0188), Washington, DC 20503.

1. AGENCY USE ONLY <i>(Leave blank)</i>			2. REPORT DATE	3. REPORT TYPE AND DATES COVERED	
			November 1996	Final, Dec 95 - Feb 96	
4. TITLE AND SUBTITLE			Investigation of Surface Intergranular Attack and Its Effects on the Fatigue Properties of AM355 Stainless Steel		5. FUNDING NUMBERS
					PR: 1L162618AH80
6. AUTHOR(S)			Scott Grendahl and Victor Champagne		
7. PERFORMING ORGANIZATION NAME(S) AND ADDRESS(ES)			U.S. Army Research Laboratory ATTN: AMSRL-MA-CB Aberdeen Proving Ground, MD 21005-5069		8. PERFORMING ORGANIZATION REPORT NUMBER
					ARL-TR-1238
9. SPONSORING/MONITORING AGENCY NAMES(S) AND ADDRESS(ES)			U.S. Army Aviation and Troop Command 4300 Goodfellow Blvd. St. Louis, MO 63120-1798		10. SPONSORING/MONITORING AGENCY REPORT NUMBER
11. SUPPLEMENTARY NOTES					
12a. DISTRIBUTION/AVAILABILITY STATEMENT			12b. DISTRIBUTION CODE		
Approved for public release; distribution is unlimited.					
13. ABSTRACT <i>(Maximum 200 words)</i>					
A critical flight safety component fabricated from AM355, a semiaustenitic precipitation hardenable stainless steel, from an Army attack helicopter failed catastrophically in service. The U.S. Army Research Laboratory (ARL) performed an in-depth metallurgical analysis of the broken component, which revealed that the premature failure was attributable to fatigue. Further analysis of material taken from various stages of processing revealed an intergranular surface attack that ARL determined to be caused by acid pickling during primary processing. ARL hypothesized that the surface intergranular attack may have led to premature crack initiation due to the breakdown of the protective passive layer or the stress concentration effect of the attack. This study was conducted to quantify the effects of varying degrees of surface intergranular attack on the fatigue properties of the material. Fatigue specimens were machined from actual components taken from inventory and from fielded components and were subsequently categorized into four groups which described the degree or severity of attack based on appearance and depth measurement: none, light, moderate, and heavy. Fatigue test data showed a direct relationship between the number of cycles to failure and the severity of surface intergranular attack. ARL recommended to control the amount of surface intergranular attack or to remove it altogether with a light sanding operation.					
14. SUBJECT TERMS			15. NUMBER OF PAGES		
			47		
AM355, stainless steel, fatigue, pickling			16. PRICE CODE		
17. SECURITY CLASSIFICATION OF REPORT		18. SECURITY CLASSIFICATION OF THIS PAGE		19. SECURITY CLASSIFICATION OF ABSTRACT	
UNCLASSIFIED		UNCLASSIFIED		UNCLASSIFIED	
				20. LIMITATION OF ABSTRACT	
				UL	

**INTENTIONALLY LEFT BLANK.**

## ACKNOWLEDGMENTS

The authors would like to acknowledge Brad Waterson, Worcester Polytechnic Institute, Worcester, MA, for making significant contributions in acquiring the data expressed within this report.

**INTENTIONALLY LEFT BLANK.**

## TABLE OF CONTENTS

	<u>Page</u>
ACKNOWLEDGMENTS .....	iii
LIST OF FIGURES .....	vii
LIST OF TABLES .....	ix
1. INTRODUCTION .....	1
2. BACKGROUND .....	1
3. TEST PLAN .....	1
4. OPTICAL MICROSCOPY .....	4
5. SCANNING ELECTRON MICROSCOPY .....	5
6. FATIGUE AND TENSILE RESULTS .....	6
7. DISCUSSION .....	14
8. CONCLUSIONS .....	15
9. RECOMMENDATIONS .....	15
DISTRIBUTION LIST .....	41

**INTENTIONALLY LEFT BLANK.**

## LIST OF FIGURES

<u>Figure</u>	<u>Page</u>
1. SEM fractograph of 11L from SP #7888 showing an edge origin. Mag. 250 $\times$ . ....	16
2. SEM fractograph of 11L from SP #7888 showing edge scratches. Mag. 250 $\times$ . ....	16
3. SEM fractograph of SP #7888 11L showing the scratch root origin. Mag. 1000 $\times$ . ....	17
4. SEM fractograph of SP #7888 11L showing lack of intergranular edge. Mag. 750 $\times$ . ....	17
5. SEM fractograph of 10L from SP #6800 showing thumbnail origin. Mag. 50 $\times$ . ....	18
6. SEM fractograph of SP #6800 10L showing the origin. Mag. 250 $\times$ . ....	18
7. SEM fractograph of SP #6800 10L showing the surface pit origin. Mag. 250 $\times$ . ....	19
8. SEM fractograph of SP #6800 10L showing lack of intergranular edge. Mag. 1000 $\times$ . ....	19
9. SEM fractograph of Trial R12 showing an edge origin. Mag. 250 $\times$ . ....	20
10. SEM fractograph of Trial R12 showing edge scratches. Mag. 250 $\times$ . ....	20
11. SEM fractograph of Trial R12 showing an edge scratch origin. Mag. 1000 $\times$ . ....	21
12. SEM fractograph of Trial R12 showing fatigue by edge intergranular. Mag. 100 $\times$ . ....	21
13. SEM fractograph of Trial R12 showing removed grains on edge. Mag. 750 $\times$ . ....	22
14. SEM fractograph of low-cost AR showing surface failure origin. Mag. 250 $\times$ ....	22
15. SEM fractograph of low-cost AR showing location of surface origin. Mag. 100 $\times$ . ....	23
16. SEM fractograph of low-cost AR showing intergranular at origin. Mag. 1000 $\times$ . ....	23
17. SEM fractograph of low-cost AR intergranular attack near the origin. Mag. 500 $\times$ . ....	24
18. SEM fractograph of low-cost AR intergranular morphology at origin. Mag. 3000 $\times$ . ....	24
19. SEM fractograph of low-cost AR removed edge grains and secondary cracking origin. Mag. 500 $\times$ . ....	25
20. AM355 axial fatigue test - S-N curve; Kt = 1; T = 0.014; G = 0.660; R = 0.05. ....	26
21. AM355 axial fatigue test - S-N curve; Kt = 1; T = 0.014; G = 0.660; R = 0.05; best-fit curves. ....	27

<u>Figure</u>	<u>Page</u>
22. AM355 axial fatigue test - S-N curve; $K_t = 1$ ; $T = 0.014$ ; $G = 0.660$ ; $R = 0.05$ ; trial. ....	28
23. AM355 axial fatigue test - S-N curve; $K_t = 1$ ; $T = 0.014$ ; $G = 0.660$ ; $R = 0.05$ ; trial best fit. ....	29
24. AM355 axial fatigue test - S-N curve; $K_t = 1$ ; $T = 0.014$ ; $G = 0.660$ ; $R = 0.05$ ; KSD. ....	30
25. AM355 axial fatigue test - S-N curve; $K_t = 1$ ; $T = 0.014$ ; $G = 0.660$ ; $R = 0.05$ ; KSD best fit. ....	31
26. AM355 axial fatigue test - S-N curve; $K_t = 1$ ; $T = 0.014$ ; $G = 0.660$ ; $R = 0.05$ ; SP #6800. ....	32
27. AM355 axial fatigue test - S-N curve; $K_t = 1$ ; $T = 0.014$ ; $G = 0.660$ ; $R = 0.05$ ; SP #6800 best fit. ....	33
28. AM355 axial fatigue test - S-N curve; $K_t = 1$ ; $T = 0.014$ ; $G = 0.660$ ; $R = 0.05$ ; SP #7888. ....	34
29. AM355 axial fatigue test - S-N curve; $K_t = 1$ ; $T = 0.014$ ; $G = 0.660$ ; $R = 0.05$ ; SP #7888 best fit. ....	35
30. AM355 axial fatigue test - S-N curve; $K_t = 1$ ; $T = 0.014$ ; $G = 0.660$ ; $R = 0.05$ ; least-squares regression fit. ....	36
31. Least-squares regression fit. ....	37
32. AM355 axial fatigue test - S-N curve; $K_t = 1$ ; $T = 0.014$ ; $G = 0.660$ ; $R = 0.05$ ; power law fit. ....	38
33. Power law fit. ....	39

## LIST OF TABLES

<u>Table</u>	<u>Page</u>
1. Laminate Material Test Plan .....	2
2. Laminate Measurement Data .....	3
3. Laminate Failure Locations .....	4
4. Laminate Fatigue Testing Results .....	7
5. Best-Fit Approximations .....	8
6. Laminate Least-Squares Regression Fit .....	13
7. Laminate Mechanical Test Data .....	14

**INTENTIONALLY LEFT BLANK.**

## 1. INTRODUCTION

The purpose of this study was to determine if the fatigue properties of AM355 stainless steel are adversely affected by an intergranular surface attack caused by "pickling" during primary material processing.

## 2. BACKGROUND

The U.S. Army Aviation and Troop Command (ATCOM) visited the KSD Corporation in response to a surface condition observed on Apache strap pack laminate material, AM355 stainless steel. The material contained small black spots, which appeared during the manufacturing of the strap pack. As a result of this visit, ATCOM requested an analysis of these anomalies from the Materials Directorate of the U.S. Army Research Laboratory (ARL). ARL concluded that the anomalies were caused by entrapped particles on the surface that fretted during manufacturing operations, causing the black spots. The particles had been lodged within areas of surface intergranular attack. As a direct result of that analysis,<sup>1</sup> ATCOM requested ARL to investigate the intergranular surface attack that was the precursor and probable root-cause of the surface anomaly in more detail. ARL was informed that this condition was inherent to the primary processing of AM355 by Allegheny Ludlum and existed on the material before the assembly of the strap pack laminates. Further investigation revealed that the surface intergranular attack on the AM355 laminate material was most likely the result of a prior pickling operation performed during primary processing of the material. The severity of the intergranular attack was not observed during prior ARL analyses (although a similar condition on a much lesser scale was detected on previously inspected strap packs), and its consequences were not known. Until recently, this condition was being removed from some strap packs by a surface finishing operation performed by McDonnell Douglas Helicopter Systems (MDHS). ARL proceeded to perform fatigue and tensile testing of the AM355 laminate material to explore the effects of the surface intergranular attack. A detailed test plan was formulated including material received by ARL from previous investigations of the Main Rotor Strap Pack.

## 3. TEST PLAN

The test plan included selecting material with varying degrees of attack, including heavy attack, moderate to heavy attack, moderate attack, and only slightly attacked to void of attack. ARL received three sets of

---

<sup>1</sup>Grendahl, S., and V. K. Champagne. "Analysis of AH-64 Apache Strap Pack Laminate Surface Anomalies." U.S. Army Research Laboratory, 26 October 1995.

laminates upon which fatigue and tensile tests were to be performed. The material was designated as "KSD" from KSD corporation, "Trial" from MDHS, and "Low Cost," also from MDHS (that consisted of unprocessed laminates—meaning not reamed, end-milled, or edge broken). In addition, laminates were tested from two strap packs previously received by ARL during an unrelated investigation. Strap pack laminates were taken from SP #6800, that had 614 prior service hours, and from SP #7888, that had 248 prior service hours. These strap laminates were selected to represent "virgin" material since they had few flight hours and thus limited internal mechanical damage. Table 1 outlines the test plan created to assess the effects of the intergranular surface condition on the tensile and fatigue properties of the material.

Table 1. Laminate Material Test Plan

Material	IG Condition	Fatigue (Specs.)	Tensile (Specs.)
KSD	Moderate-Heavy	10	3
Trial	Moderate	16	2
Low Cost	Heavy	2	1
SP #6800	Very Light - None	7	1
SP #7888	Very Light - None	7	1

Each specimen was precisely measured with a Mitutoyo Mikematic Micrometer Model #MK 100E. The results of these measurements are presented in Table 2. ARL was provided with baseline cyclic fatigue curves for the AM355 material. The results of the testing can be observed in tabular form in Table 4 and in graphical form in Figures 20–29.

**Table 2. Laminate Measurement Data**

Specimen	Thickness					Average	Width					Average	Cross-Sec. Area
TR 1	0.01400	0.01405	0.01410	0.01410	0.01410	<b>0.01407</b>	0.66100	0.66110	0.66105	0.66115	0.66110	<b>0.66108</b>	<b>0.0093014</b>
TL1	0.01415	0.01415	0.01415	0.01415	0.01415	<b>0.01415</b>	0.66060	0.66050	0.66055	0.66060	0.66045	<b>0.66054</b>	<b>0.0093466</b>
TR 2	0.01405	0.01400	0.01405	0.01410	0.01405	<b>0.01405</b>	0.66130	0.66135	0.66140	0.66125	0.66135	<b>0.66133</b>	<b>0.0092917</b>
TL 2	0.01415	0.01415	0.01415	0.01415	0.01415	<b>0.01415</b>	0.66085	0.66110	0.66125	0.66100	0.66120	<b>0.66108</b>	<b>0.0093543</b>
TL5	0.01405	0.01410	0.01415	0.01415	0.01410	<b>0.01411</b>	0.66110	0.66115	0.66105	0.66100	0.66115	<b>0.66109</b>	<b>0.0093280</b>
TR 5	0.01410	0.01415	0.01405	0.01410	0.01410	<b>0.01410</b>	0.66095	0.66085	0.66105	0.66100	0.66090	<b>0.66095</b>	<b>0.0093194</b>
TR 6	0.01400	0.01405	0.01400	0.01410	0.01405	<b>0.01404</b>	0.66100	0.66105	0.66120	0.66100	0.66110	<b>0.66107</b>	<b>0.0092814</b>
TL 6	0.01405	0.01405	0.01410	0.01410	0.01405	<b>0.01407</b>	0.66085	0.66100	0.66090	0.66120	0.66110	<b>0.66093</b>	<b>0.0092993</b>
TL7	0.01410	0.01410	0.01405	0.01405	0.01405	<b>0.01407</b>	0.66100	0.66075	0.66095	0.66085	0.66108	<b>0.66108</b>	<b>0.0093014</b>
TR 7	0.01410	0.01410	0.01405	0.01410	0.01415	<b>0.01410</b>	0.66105	0.66095	0.66100	0.66090	0.66095	<b>0.66097</b>	<b>0.0093197</b>
TR 11	0.01410	0.01405	0.01410	0.01410	0.01410	<b>0.01409</b>	0.66070	0.66080	0.66075	0.66075	0.66070	<b>0.66088</b>	<b>0.0093118</b>
TL11	0.01415	0.01415	0.01415	0.01415	0.01410	<b>0.01414</b>	0.66100	0.66105	0.66095	0.66115	0.66120	<b>0.66074</b>	<b>0.0093429</b>
TR 12	0.01405	0.01405	0.01400	0.01405	0.01405	<b>0.01404</b>	0.66085	0.66090	0.66095	0.66080	0.66080	<b>0.66101</b>	<b>0.0092806</b>
TL 12	0.01415	0.01415	0.01410	0.01415	0.01415	<b>0.01414</b>	0.66100	0.66050	0.66085	0.66095	0.66060	<b>0.66117</b>	<b>0.0093489</b>
TL 14	0.01410	0.01410	0.01405	0.01410	0.01410	<b>0.01409</b>	0.66120	0.66130	0.66130	0.66125	0.66115	<b>0.66083</b>	<b>0.0093111</b>
TR 19	0.01400	0.01405	0.01405	0.01410	0.01410	<b>0.01403</b>	0.66100	0.66050	0.66085	0.66095	0.66060	<b>0.66078</b>	<b>0.0092707</b>
TL 19	0.01410	0.01410	0.01405	0.01410	0.01415	<b>0.01410</b>	0.66120	0.66130	0.66130	0.66125	0.66115	<b>0.66124</b>	<b>0.0093235</b>
TR 21	0.01410	0.01405	0.01410	0.01415	0.01405	<b>0.01409</b>	0.66100	0.66105	0.66090	0.66095	0.66095	<b>0.66097</b>	<b>0.0093131</b>
TL 21	0.01405	0.01405	0.01405	0.01410	0.01410	<b>0.01406</b>	0.66090	0.66105	0.66115	0.66100	0.66120	<b>0.66106</b>	<b>0.0092945</b>
7888 L 11	0.01410	0.01410	0.01410	0.01410	0.01410	<b>0.01410</b>	0.66130	0.66025	0.66040	0.66030	0.66025	<b>0.66030</b>	<b>0.0093102</b>
7888 R 11	0.01405	0.01410	0.01410	0.01410	0.01415	<b>0.01410</b>	0.65980	0.65960	0.65940	0.65965	0.65955	<b>0.65960</b>	<b>0.0093004</b>
7888 L 12	0.01420	0.01420	0.01415	0.01420	0.01420	<b>0.01419</b>	0.66030	0.66050	0.66035	0.66040	0.66020	<b>0.66035</b>	<b>0.0093704</b>
7888 R 12	0.01420	0.01425	0.01425	0.01420	0.01420	<b>0.01421</b>	0.66030	0.66025	0.66040	0.66025	0.66040	<b>0.66032</b>	<b>0.0093831</b>
7888 L 13	0.01415	0.01415	0.01415	0.01415	0.01420	<b>0.01416</b>	0.66010	0.66005	0.66010	0.66015	0.65980	<b>0.66004</b>	<b>0.0093462</b>
7888 R 13	0.01425	0.01420	0.01420	0.01425	0.01425	<b>0.01423</b>	0.65995	0.65975	0.65960	0.65980	0.65965	<b>0.65975</b>	<b>0.0093882</b>
6800 L 9-1	0.01400	0.01400	0.01400	0.01405	0.01400	<b>0.01401</b>	0.66060	0.66050	0.66055	0.66065	0.66060	<b>0.66058</b>	<b>0.0092547</b>
6800 L 9-2	0.01400	0.01405	0.01405	0.01400	0.01400	<b>0.01402</b>	0.66045	0.66050	0.66055	0.66040	0.66045	<b>0.66047</b>	<b>0.0092598</b>
6800 L 10	0.01400	0.01400	0.01400	0.01400	0.01400	<b>0.01400</b>	0.66075	0.66060	0.66080	0.66080	0.66060	<b>0.66071</b>	<b>0.0092499</b>
6800 R 10	0.01415	0.01405	0.01405	0.01400	0.01400	<b>0.01405</b>	0.65985	0.65990	0.66010	0.66005	0.65995	<b>0.65997</b>	<b>0.0092726</b>
6800 L 11	0.01400	0.01400	0.01420	0.01415	0.01400	<b>0.01407</b>	0.66080	0.66090	0.66095	0.66080	0.66105	<b>0.66090</b>	<b>0.0092989</b>
6800 R 11	0.01400	0.01400	0.01400	0.01410	0.01405	<b>0.01403</b>	0.65990	0.65985	0.65980	0.65995	0.65010	<b>0.65992</b>	<b>0.0092587</b>
6800 L 13	0.01400	0.01405	0.01405	0.01400	0.01400	<b>0.01402</b>	0.66045	0.66050	0.66070	0.66070	0.66075	<b>0.66062</b>	<b>0.0092619</b>
6800 L13-2	0.01395	0.01395	0.01395	0.01390	0.01395	<b>0.01399</b>	0.65960	0.65970	0.65950	0.65975	0.65995	<b>0.65970</b>	<b>0.0092292</b>
LCAL	0.01455	0.01455	0.01455	0.01455	0.01450	<b>0.01454</b>	0.66075	0.66080	0.66100	0.66085	0.66105	<b>0.66089</b>	<b>0.0096093</b>
LCBL	0.01465	0.01460	0.01465	0.01460	0.01465	<b>0.01463</b>	0.66110	0.66130	0.66150	0.66135	0.66140	<b>0.66133</b>	<b>0.0096753</b>
LCAR	0.01470	0.01470	0.01470	0.01460	0.01465	<b>0.01467</b>	0.66140	0.66135	0.66155	0.66145	0.66140	<b>0.66143</b>	<b>0.0097032</b>
KSD AR	0.01405	0.01405	0.01400	0.01400	0.01405	<b>0.01403</b>	0.66160	0.66170	0.66165	0.66140	0.66150	<b>0.66157</b>	<b>0.0092818</b>
KSD BL	0.01405	0.01405	0.01405	0.01410	0.01410	<b>0.01407</b>	0.66260	0.66270	0.66280	0.66260	0.66280	<b>0.66270</b>	<b>0.0093242</b>
KSD BR-1	0.01400	0.01405	0.01405	0.01405	0.01400	<b>0.01403</b>	0.66290	0.66280	0.66275	0.66280	0.66290	<b>0.66283</b>	<b>0.0092995</b>
KSD BR-2	0.01405	0.01400	0.01400	0.01400	0.01400	<b>0.01401</b>	0.66095	0.66085	0.66080	0.66100	0.66090	<b>0.66090</b>	<b>0.0092592</b>
KSD CL	0.01400	0.01400	0.01395	0.01400	0.01400	<b>0.01399</b>	0.66380	0.66400	0.66415	0.66380	0.66370	<b>0.66376</b>	<b>0.0092860</b>
KSD CR-1	0.01400	0.01400	0.01400	0.01405	0.01400	<b>0.01401</b>	0.66250	0.66260	0.66225	0.66230	0.66245	<b>0.66247</b>	<b>0.0092812</b>
KSD CR-2	0.01405	0.01400	0.01400	0.01390	0.01400	<b>0.01399</b>	0.66100	0.66085	0.66080	0.66095	0.66085	<b>0.66089</b>	<b>0.0092459</b>
KSD DL	0.01400	0.01400	0.01400	0.01400	0.01400	<b>0.01400</b>	0.66140	0.66120	0.66105	0.66095	0.66095	<b>0.66111</b>	<b>0.0092555</b>
KSD DR-1	0.01390	0.01395	0.01390	0.01395	0.01390	<b>0.01393</b>	0.66175	0.66180	0.66170	0.66185	0.66180	<b>0.66179</b>	<b>0.0092187</b>
KSD DR-2	0.01395	0.01400	0.01400	0.01405	0.01400	<b>0.01401</b>	0.66100	0.66120	0.66135	0.66140	0.66115	<b>0.66122</b>	<b>0.0092637</b>

#### 4. OPTICAL MICROSCOPY

The fractured halves from the fatigue and tensile testing were optically examined. The fracture origins were determined to be from either edge or surface flaws. A listing is presented in Table 3.

Table 3. Laminate Failure Locations

Specimen	Failure Location
TR 1	not failed
TL1	edge
TR 2	not failed
TL 2	edge
TL5	edge
TR 6	not failed
TL 6	edge
TL7	not failed
TR 11	edge
TL11	edge
TR 12	edge
TL 12	edge
TL 14	edge
TR 19	edge
TL 19	edge
TR 21	not failed
TL 21	not failed
7888 L 11	edge
7888 R 11	edge
7888 L 12	edge
7888 R 12	edge
7888 L 13	not failed
7888 R 13	edge
6800 L 10	surface pit
6800 R 10	edge
6800 L 11	not failed
6800 R 11	edge
LCAL	not failed
LCBL	not failed
LCAR	surface
KSD AR	edge
KSD BL	not failed
KSD BR-1	edge
KSD BR-2	edge
KSD CL	not failed
KSD CR-1	edge
KSD CR-2	edge
KSD DL	edge
KSD DR-1	edge
KSD DR-2	edge

## 5. SCANNING ELECTRON MICROSCOPY

Scanning electron microscopy was used to determine the exact nature of failure and location of the fatigue origin(s). The specimens failed predominantly from edge defects. The edge finishing performed on the specimens allowed for scratches perpendicular to the specimen length. For the specimens that failed from the edge, these scratches were the origin of fracture, as expected. Figure 1 shows specimen 11L from Strap Pack #7888 with an edge fracture origin (arrow denotes origin). Further investigation revealed scratches on the edge as a result of the finishing procedure, as shown in Figure 2. Upon closer examination, it was observed that the root of a scratch on the edge of the specimen was the origin of fracture. The origin is depicted at higher magnification in Figure 3. Specimens from Strap Pack #7888 did not display any intergranular attack of the surface, and consequently, the edge of the fatigue specimen did not contain any intergranular morphology along its edges. The surface edge of specimen #7888 11L can be observed in Figure 4.

Figure 5 shows specimen 10L from Strap Pack #6800. A "thumbnail" crack region can be seen containing radial lines that indicate the origin of the fracture. The origin is shown at higher magnification in Figure 6. Since both Strap Packs #7888 and #6800 had seen prior service, it was expected that pitting and subsequent surface failures would be observed. Specimen 10L from #6800 failed from a surface pit as depicted in Figure 7. There was no intergranular fracture morphology along the edges of the specimens from Strap Pack #6800. This was expected, since Strap Pack #6800 had minimal to no surface intergranular attack. Figure 8 depicts the edge of specimen 10L from #6800 at high magnification. For comparison, the failures of the specimens with some surface intergranular attack were examined.

Figure 9 shows the edge failure of "Trial" Strap Pack specimen R12 (arrow denotes origin). This edge failure was caused by surface scratches induced during the edge finishing process, shown in Figure 10 and at higher magnification in Figure 11. However, the "Trial" strap-pack laminates contained characteristics near the surface not witnessed on the strap packs that had experienced prior service (#7888 and #6800). The intergranular attack of the surface of these specimens (categorized as moderate attack) allowed the fatigue crack front to progress along an intergranular network near the surface. Figure 12 shows the fatigue crack following the intergranular network near the surface of the specimens (arrows denote intergranular morphology along edges).

Figure 13 depicts the edge of specimen "Trial" R12. It can clearly be seen that the intergranular surface attack allows the crack to progress in an intergranular mode near the surface. It can be observed in Figure 13 that a few grains were removed entirely as the crack progressed around them. There were also significant secondary cracks on the surface of the specimen adjacent to the main crack front.

Figure 14 shows the origin area on specimen AR from the Strap Pack labeled "low cost." The intergranular condition of these laminates was the worst or the deepest surface attack observed. This specimen failed from a surface flaw. Figure 15 shows the proximity of the surface flaw origin to the nearest edge. Closer examination revealed an intergranular morphology at the origin (shown in Figure 16). The surface intergranular condition near the origin is shown in Figure 17. The depth and severity of this attack can easily be observed. The intergranular morphology at the origin is depicted at high magnification in Figure 18. The effect of the heavy intergranular surface attack can be observed in Figure 19 as removed grains and severe secondary cracking are clearly evident as well as intergranular morphology along the edge. The specimens that did not contain this intergranular network did not have the crack front progressing in an intergranular mode near the surface. The crack front progressed by a transgranular mode until transitioning to complete ductility.

## 6. FATIGUE AND TENSILE RESULTS

The results of the fatigue tests are presented in Table 4 and in graphical format in Figures 20–33. Figures 20–29 show the data plotted with "best-fit" approximations according to the equation  $y = (a + b \ln(x) + c/x^2)$ , which was acquired from curve-fitting software. A least-squares regression fit is applied in Figures 30 and 31. Finally, a power law fit is applied to the data in Figures 32 and 33.

The "best-fit" approximations can be previewed in Table 5.

**Table 4. Laminate Fatigue Testing Results**

Specimen Designation	Scribe Designation	Cyclic Stress Amplitude	Cross-Sectional Area	Projected Loads ( Pounds)			Cyclic Stress	Cycles To Failure
				Max.	Min.	Mean		
6800 9L-1	9L-1	67.5	0.0092547	1314.3	65.7	690	624.4	55565
6800 9L-2	9L-2	67.4	0.0092598	1314.3	65.7	690	624.4	47986
6800 L 10	L 10	74.9	0.0092499	1459	73.0	766.0	693	88805
6800 R 10	R 10	69.8	0.0092726	1362.0	68.0	715.0	647	71278
6800 R 11	R 11	79.8	0.0092587	1552.0	77.6	814.8	814.8	37649
6800 13L-1	13L-1	64.9	0.0092619	1265.4	62.9	664.2	601.3	3 Million
6800 13L-2	13L-2	65	0.0092292	1264.0	62.8	663.6	600.6	3 Million
7888 11 L	11 L	71.9	0.0093102	1408.5	70.4	739.3	669.2	43237
7888 11 R	11 R	79.5	0.0093004	1552.0	77.6	815.0	739.2	23394
7888 12 L	12 L	71.5	0.0093704	1409.7	70.5	740.1	669.6	99601
7888 12 R	12 R	73.8	0.0093831	1459.0	73.0	766.0	693	40925
7888 13 L	13 L	69.2	0.0093462	1362.0	68.0	715.0	647	3 Million
7888 13 R	13 R	71.3	0.0093882	1409.7	70.5	740.1	669.6	87210
KSD AR	AR	64.9	0.0092818	1269.0	63.4	665.3	602.8	165352
KSD BL	BL	64.6	0.0093242	1269.0	63.4	665.3	602.8	3 Million
KSD BR-1	BR-1	72.2	0.0092995	1413.2	70.7	742.0	671.3	60221
KSD BR-2	BR-2	86.9	0.0092592	1649.1	85.9	889.0	804.6	17101
KSD CL	CL	62.7	0.0092860	1225.7	80.9	643.3	582.4	3 Million
KSD CR-1	CR-1	77	0.0092812	1505.5	75.1	790.3	715.2	35513
KSD CR-2	CR-2	67.5	0.0092459	1314.8	66.0	690.4	624.4	28540
KSD DL	DL	67.5	0.0092555	1314.8	66.0	690.4	624.4	84361
KSD DR-1	DR-1	68	0.0092187	1319.2	66.2	692.7	626.5	56138
KSD DR-2	DR-2	65.1	0.0092637	1269.0	63.4	665.3	602.8	291466
LC 802757AL	LCAL	untested	0.0096093					
LC 802757AR	LCAR	66.7	0.0097032	1362.0	68.0	715.0	647	53190
LC 802757BL	LCBL	57.3	0.0096753	1167.0	58.4	612.8	554.4	3 Million
Trial L1	TL1	69.2	0.0093466	1362.0	68.0	715.0	647	44611
Trial R1	TR1	57	0.0093014	119.0	56.4	587.2	531	3 Million
Trial L2	TL2	64.3	0.0093543	1266.3	63.3	665.0	601.5	70422
Trial R2	TR2	64.7	0.0092917	1266.3	63.3	665.0	601.5	3 Million
Trial L5	TL5	66.9	0.0093280	1314.3	65.7	690.0	624.6	87941
Trial R5	TR5	62	0.0093194	1217.0	60.9	639.0	578	93117
Trial L6	TL6	62.1	0.0092993	1217.0	60.9	639.0	578	62477
Trial R6	TR6	54.2	0.0092814	1069.9	53.6	561.3	508.2	3 Million
Trial L7	TL7	59.7	0.0093014	1168.0	58.3	613.3	555	3 Million
Trial R7	TR7	62	0.0093197	1217.0	60.9	639.0	578	137717
Trial L11	TL11	79.6	0.0092806	1552.0	77.6	815.0	739.2	31960
Trial R11	TR11	59.5	0.0093118	1167.0	58.4	612.8	554.4	155895
Trial R12	TR12	82	0.0093489	1595.0	250.0	916.8	???	42218
Trial L14	TL14	89.3	0.0093111	1750.7	87.5	919.1	831.6	10986
Trial L19	TL19	79.3	0.0093235	1552.0	77.6	815.0	739.2	66804
Trial R19	TR19	69.8	0.0092707	1362.0	68.0	715.0	647	77780

Table 5. Best-Fit Approximations

Trial Data									
Date	Apr 3, 1996	X Y Range	Cycles	Cyclic Stress Amp.	Y Predicted	Y Residual	Y % Residual	95% Confidence Limits	95% Prediction Limits
Time	4:16 PM	1	10986	89.3	90.52338249	-1.223382189	-1.37046466	76.913061477	104.134585
XY Points	16	2	31960	79.6	72.80931083	6.79069177	8.53101972	68.05969596	77.5589196
XY Minimum	10986	3	42218	82	71.16704844	10.83295116	13.21091066	66.580763835	75.7533428
XY Maximum	30000000	4	44611	69.2	70.89021811	-1.69021814	-2.44251176	66.3400015	75.4404348
XY Range	2989014	5	62447	62.1	69.4242063	-7.32420627	-11.794213	65.12709624	73.7213163
XY Mean	805118.63	6	66804	79.3	69.1642139	10.1357861	12.7815713	64.92201239	73.4064155
XY StdDev	13092622	7	70422	64.3	68.966645	-4.66664495	-7.25761268	64.76759483	73.1656951
XY Median	82860.5	8	77780	69.8	68.6052348	1.19376524	1.7026538	64.48808451	72.724385
XY@Ymin	3000000	9	87941	66.9	68.1787917	-1.27879168	-1.911149728	64.15781676	72.1997366
XY@Ymax	10986	10	93117	62	67.985274	-5.985274	-9.653306775	64.007782325	53.9227813
XY@Y Range	2989014	11	137717	62	67.7271775	-4.72717499	-7.62447579	53.74147155	82.2290765
Yavg@Yma	10986	12	155895	59.5	66.3451166	-6.84511658	-11.5043976	62.99399558	52.54964127
XY@50Y	179979.82	13	31E+06	57	57.7029858	-0.70298579	-1.23330384	62.662272769	70.0275055
XY@50Y	0	14	31E+06	54.2	57.7029858	-3.50298579	-50.97417408	64.4318275	52.1808721
XY@50Y	0	15	31E+06	59.7	57.7029858	1.99701421	3.34508243	64.4318275	80.5093611
XY@25Y	-1356704	16	31E+06	64.7	57.7029858	6.99701421	10.81455306	50.97417408	72.9457921
XY@75Y	-1733626								
XYwavenmin	30000000				Equation #	75			
XYwaveRang	3978028				Equation	y=(a1*ln(x))+c*x^2)			
Y Minimum	54.2				r2	0.65333085332022			
Y Maximum	89.3				Ft Std Err	6.32317907			
Y Range	35.1				F-stat	12.2486537			
Y Mean	67.6				Confidence	95			
Y StdDev	9.9974663				A	100.873859			
Y Median	64.5				A Std Err	12.3988636			
Y@Xmin	89.3				A t	8.1357302			
Y@Xmax	64.7				A Conf limits	74.0547838			
Y@X Range	24.6				B	127.692917			
F1					B Std Err	-2.8946453			
F2					C	0.9990758			
F3					C Std Err	20014190722			
					C	-0.733361970			
					C1	905851488			
					C Conf.limits	2.20943396			
					C1	42038615			
					C Conf.limits	3960799399			

**Table 5. Best-Fit Approximations (continued)**

KSD Data											
Date	Apr 3, 1996	Y Pt #	Cycles	Cyclic Stress Amp.	Y Predicted	Y Residual	Y % Residual	95% Confidence Limits		95% Prediction Limits	
Time	3:54 PM	1	17101	86.9	85.84216414	1.057533586	1.21695726	77.657673	94.0272553	73.98158823	97.70334
X Y Points	10 2	28540	67.5	74.24694383	-6.74694383	-9.99547234	70.588821558	77.9056721	61.91549894	83.5783887	
X Minimum	17101 3	35513	77	71.83096386	5.16903614	6.71303395	68.24408338	75.4178443	62.52745469	81.134473	
X Maximum	30000000 4	56138	68	68.97174418	-0.97174418	-1.42903556	65.27115861	72.6723297	59.62380832	78.31968	
X Range	2982899 5	60221	72.2	68.69197899	3.50802101	4.85875486	64.99840795	72.38555	59.34681777	78.0371402	
X Mean	673889.2 6	84361	67.5	67.67434578	-0.17434578	-0.25829005	64.09561955	71.253072	58.37397736	76.9747142	
X StdDev	1228710.2 7	2E+05	64.9	66.48275179	-1.58275179	-2.43875468	63.23709169	69.7284119	57.30539483	75.6601087	
X Median	72291 8	3E+05	65.1	65.79651181	-0.69651181	-1.06991062	62.61314406	68.9798796	56.64099973	74.9520239	
X@Ymin	30000000 9	3E+06	62.7	63.43114781	-0.73114781	-1.16610496	57.64263841	69.2196572	53.07757778	73.787178	
X@Ymax	17101 10	3E+06	64.6	63.43114781	1.16885219	1.80936872	57.64263841	69.2196572	53.07757778	73.787178	
X@Y Range	2982899										
Xavg@Yma	17101										
X@Yma	48867.246			Equation #	75						
X@50Y	0			Equation	$y = (a \cdot b \ln(x) + c)/x^2$						
Xfit@50Y	0			R <sup>2</sup>	0.81010231485						
X@25Y	83022.681			Fit StdErr	3.616045331						
X@75Y	22444.679			F-stat	15.12695217						
Xwavenin	165352			Confidence	95						
Xwavenax	17101			A	78.18431705						
XwaveRang	296502			A StdErr	10.46819882						
Y Minimum	62.7			A t	7.468745905						
Y Maximum	86.9			A Conflimits	53.333474788						
Y Range	24.2			B	103.0351592						
Y Mean	69.64			B StdErr	-0.989245666						
Y StdDev	7.3569619			B t	0.832506106						
Y Median	67.5			B Conflimits	-1.188274367						
Y@Xmin	86.9			C	-2.965562529						
Y@Xmax	64.6			C StdErr	0.987071197						
Y@X Range	22.3			C t	5059348423						
F1				C Conflimits	1430330189						
F2				C t	3.537189148						
F3				C Conflimits	1663834983						
					8454861863						

Table 5. Best-Fit Approximations (continued)

SP 6800 Data									
Date	Apr 3, 1996	Y Pt	Cycles	Cyclic Stress Amp	Y Predicted	Y Residual	Y % Residual	95% Confidence Limits	95% Prediction Limits
Date	Apr 3, 1996	Y Pt	Cycles	Cyclic Stress Amp	Y Predicted	Y Residual	Y % Residual	95% Confidence Limits	95% Prediction Limits
Time	3:50 PM	1	37649	79.8	75.707988	4.0020119	5.12783441	63.59684508	87.819131
XY Points		2	47986	67.4	72.716857	-5.316857	-7.888512	66.19960045	57.69724768
X Minimum	37649	3	55565	67.5	71.464316	-3.964316	-5.87306	65.13697606	56.52613434
X Maximum	3000000	4	71278	69.8	69.563884	-0.163884	-0.2347913	62.20851661	54.36709746
X Range	2962351	5	88805	74.9	69.076474	5.8235256	7.75306759	60.29513336	52.94495298
X Mean	900183.29	6	3000000	64.9	65.18324	-0.28324	-0.4395073	55.62242757	48.6153453
X StdDev	1434542	7	3000000	65	65.18324	-0.18324	-0.284985	55.62242757	48.6153453
X Median	71278								
X@Ymin	3000000			Equation #	75				
X@Ymax	37649			Equation	$y=(a+b\ln(x)+c/x^2)$				
X@Y Range	2962351			i2	0.484974393637				
Xavg@Ymin	37649			Fit StdErr	4.867387442				
X@50Y	85406.43			F-stat	1.883302064				
Xl@50Y	0			Confidence	95				
Xrt@50Y	0			A	76.10283311				
X@25Y	95127.13			A StdErr	22.1994415				
X@75Y	83100.338			A t	3.4284179				
Xwavenin	3000000			A Conflimit	14.39186865				
Xwavenax	37649				137.8377976				
Xwave Rang	5924702			B	-0.732107788				
Y Minimum	64.9			B StdErr	1.6192833003				
Y Maximum	79.8			B t	-0.452118491				
Y Range	14.9			B Conflimit	-5.233460486				
Y Mean	69.9			C	3.769244909				
Y StdDev	5.538511			C StdErr	10373853591				
Y Median	67.5			C	12378045462				
Y@Xmin	79.8			C l	0.838084948				
Y@Xmax	65			C Conflimit	-24035170787				
Y@X Range	14.8			F1	44782877969				
				F2					
				F3					

**Table 5. Best-Fit Approximations (continued)**

<b>SP 7888 Data</b>											
Date	Apr 3, 1996	X Y Pt #		Cycles	Cyclic Stress Amp.	Y Predicted	Y Residual	Y % Residual	95% Confidence	Limits	
Time	3:53 PM	1	23394	79.5	79.29240429	0.20759571	0.26112668	76.69187029	81.8929383		
XY Points	6	2	40925	73.8	73.46132158	0.33867842	0.45891384	72.14551735	74.7771258		
X Minimum	23394	3	43237	71.9	73.15788799	-1.25788799	-1.74949651	71.82547342	74.4903026		
X Maximum	2758892	4	87210	71.3	71.07374405	0.22625595	0.31732952	69.59244974	72.5550384		
X Range	2735498	5	99601	71.5	70.88889903	0.61110097	0.85468667	69.41440419	72.3633939		
X Mean	508876.5	6	3E+06	69.2	69.32574305	-0.12574305	-0.18170961	66.65739861	71.9940875		
X StdDev	1102666.843										
X Median	65223.5				Equation #	75					
X@Ymin	2758892				Equation	$y = (a + b \ln(x)) / c/x^2$					
X@Ymax	23394				r2	0.965700576268					
X@Y Range	2735498				Fit StdErr	0.852550819					
Xavg@Ymax	23394				t-stat	42.23251317					
X@50Y	39945.37031				Confidence	95					
Xlt@50Y	0				A	74.24178267					
Xrt@50Y	0				A StdErr	3.565218021					
X@25Y	69868.27089				A t	20.82391097					
X@75Y	33393.63848				A ConfLimits	62.97983665					
Xwavenin	2758892				B	85.50372869					
Xwavenax	23394				B StdErr	-0.331525958					
Xwave Range	5470996				B t	0.286245771					
Y Minimum	69.2				B ConfLimits	-1.158186394					
Y Maximum	79.5				C	-1.235729966					
Y Range	10.3				C StdErr	0.572678051					
Y Mean	72.86666667				C t	4.589401917					
Y StdDev	3.565763125				C ConfLimits	720339021.3					
Y Median	71.7				F1	6.371169381					
Y@Xmin	79.5				F2	23.13967672					
Y@Xmax	69.2				F3	6864836162					
Y@X Range	10.3										

The power law fits used can be previewed below:

- Power Law Fit for Trial Data

Fit 6: Power,  $\log(Y) = B * \log(X) + A$

Equation:  $\log(Y) = -0.0569387 * \log(X) + 4.88673$

Alternate equation:

$Y = \text{pow}(X, -0.0569387) * 132.519$

Number of data points used = 16

Average  $\log(X) = 11.9926$

Average  $\log(Y) = 4.20389$

Regression sum of squares = 0.165529

Residual sum of squares = 0.137835

Coef. of determination,  $R^2 = 0.545645$

Residual mean square,  $\hat{\Sigma}^2 = 0.00984536$

- Power Law Fit for KSD Data

Fit 8: Power,  $\log(Y) = B * \log(X) + A$

Equation:  $\log(Y) = -0.0387338 * \log(X) + 4.69652$

Alternate equation:

$Y = \text{pow}(X, -0.0387338) * 109.566$

Number of data points used = 10

Average  $\log(X) = 11.8195$

Average  $\log(Y) = 4.23871$

Regression sum of squares = 0.0449737

Residual sum of squares = 0.0439293

Coef. of determination,  $R^2 = 0.505874$

Residual mean square,  $\hat{\Sigma}^2 = 0.00549117$

- Power Law Fit for SP #6800 Data

Fit 7: Power,  $\log(Y) = B * \log(X) + A$

Equation:  $\log(Y) = -0.025433 * \log(X) + 4.55198$

Alternate equation:

$Y = \text{pow}(X, -0.025433) * 94.8204$

Number of data points used = 7

Average  $\log(X) = 12.091$

Average  $\log(Y) = 4.24447$

Regression sum of squares = 0.0147251

Residual sum of squares = 0.0208858

Coef. of determination,  $R^2 = 0.413501$

Residual mean square,  $\hat{\Sigma}^2 = 0.00417716$

- Power Law Fit for SP #7888 Data

Fit 9: Power,  $\log(Y) = B * \log(X) + A$

Equation:  $\log(Y) = -0.0201549 * \log(X) + 4.51968$

Alternate equation:

$Y = \text{pow}(X, -0.0201549) * 91.8061$

Number of data points used = 6

Average  $\log(X) = 11.5116$

Average  $\log(Y) = 4.28766$

Regression sum of squares = 0.00594523

Residual sum of squares = 0.005477

Coef. of determination,  $R^2 = 0.520496$

Residual mean square,  $\hat{\Sigma}^2 = 0.00136925$

The least-squares regression used can be previewed in Table 6.

Table 6. Laminate Least-Squares Regression Fit

Specimen Designation	Scribe Desig.	Cyclic Stress Amplitude (KSI)	Cycles to Failure	$S^2$	$\log N$				Actual Stress	Projected Fatigue Life
6800 R11	R11	79.8	37649	6368.04	365.145125	4.57575345	Sum (LogN)	36.7573	A1= 11.957311	79.8 20009.15906
6800 L10	L10	74.9	88805	5610.01	370.637963	4.94843742	Sum( $S^2$ )	34386.11	A2= -0.095941	74.9 59066.21501
6800 R10	R10	69.8	71278	4872.04	338.736294	4.85295551	Sum(S)	489.3		69.8 182237.4472
6800 9L-1	9L-1	67.5	55565	4556.25	320.274089	4.74480132	Sum(LogN)	2551.679		67.5 302901.6535
6800 9L-2	9L-2	67.4	47986	4542.76	315.507121	4.68111455	(Sum S) $^2$	239414.5		67.4 309667.5741
6800 13L-1	13L-1	64.9	3.00E+06	4212.01	420.365169	6.47712125	n	7		64.9 537957.4529
6800 13L-2	13L-2	65	3.00E+06	4225	421.012882	6.47712125				65 526203.6312
7888 I1R	I1R	79.5	23394	6320.25	347.343807	4.36910449	Sum (LogN)	30.0329	A1= 13768235	79.5 21380.16734
7888 I2R	I2R	73.8	40925	5446.44	340.364765	4.61198869	Sum( $S^2$ )	31920.88	A2= 2188.3973	73.8 75313.72158
7888 I1L	I1L	71.9	43237	5169.61	333.318014	4.63585555	Sum(S)	437.2		71.9 114593.9733
7888 I2L	I2L	71.5	99601	5112.25	357.375854	4.9982637	(Sum S) $^2$	191143.8		71.5 125180.9172
7888 I3R	I3R	71.3	87210	5083.69	352.262376	4.94056629	n	6		71.3 130835.7129
7888 I3L	I3L	69.2	3.00E+06	4788.64	448.216791	6.47712125				69.2 208066.4945
KSD BR-2	BR-2	86.9	17101	7551.61	367.849569	4.23302151	Sum (LogN)	51.33125	A1= 10.310741	86.9 7077.39215
KSD CR-1	CR-1	77	35513	5929	350.379827	4.55038736	Sum( $S^2$ )	48984.42	A2= -0.074348	77 38540.86325
KSD BR-1	BR-1	72.2	60221	5212.84	345.097803	4.77974796	Sum(S)	696.4		72.2 87658.34801
KSD CR-2	CR-2	67.5	28540	4556.25	300.743143	4.45545397	Sum(LogN)	3538.491		67.5 195988.3675
KSD DL	DL	67.5	84361	4556.25	332.514566	4.92614172	(Sum S) $^2$	484973		67.5 195988.3675
KSD DR-1	DR-1	68	56138	4624	322.949472	4.74925694	n	10		68 179910.3486
KSD AR	AR	64.9	165352	4212.01	338.674773	5.21840945				64.9 305869.2918
KSD BL	BL	64.6	3.00E+06	4173.16	418.422033	6.47712125				64.6 321988.5051
KSD DR-2	DR-2	65.1	291466	4238.01	355.744672	5.4645879				65.1 295573.9922
KSD CL	CL	62.7	3.00E+06	3931.29	406.115503	6.47712125				62.7 445761.0722
Trial I L14	TL14	89.3	10986	7974.49	360.846976	4.04083959	Sum (LogN)	83.33301	A1= 9.126935	89.3 8920.974943
Trial I R12	TR12	82	42218	6724	379.290808	4.62549766	Sum( $S^2$ )	74615.4	A2= -0.057968	82 23636.17014
Trial I L11	TL11	79.6	31960	6336.16	358.566699	4.50460677	Sum(S)	1081.6		79.6 32561.15319
Trial I L19	TL19	79.3	66804	6288.49	382.606836	4.82480247	Sum(LogN)	5546.404		79.3 33891.44698
Trial I L1	TL1	69.2	44611	4788.64	321.741384	4.64944196	(Sum S) $^2$	1169859		69.2 130486.2392
Trial I R19	TR19	69.8	77780	4872.04	341.382582	4.89086794	n	16		69.8 120443.6792
Trial I L5	TL5	66.9	87941	4475.61	330.766405	4.9441914				66.9 177374.2504
Trial I L2	TL2	64.3	70422	4134.49	311.707647	4.84770835				64.3 250961.3252
Trial I R2	TR2	64.7	3.00E+06	4186.09	419.069745	6.47712125				64.7 237913.8294
Trial I L6	TL6	62.1	62477	3856.41	297.814222	4.79572017				62.1 336616.8977
Trial I R5	TR5	62	93117	3844	308.079796	4.96902898				62 341140.0361
Trial I R7	TR7	62	137717	3844	318.617228	5.13898755				62 341140.0361
Trial I L7	TL7	59.7	3.00E+06	3564.09	386.684139	6.47712125				59.7 463722.9427
Trial I R11	TR11	59.5	155895	3540.25	308.973515	5.19283219				59.5 476268.8075
Trial I R1	TR1	57	3.00E+06	3249	369.195912	6.47712125				57 664923.354
Trial I R6	TR6	54.2	3.00E+06	2937.64	351.059972	6.47712125				54.2 966231.8934

Least Squares Equations Used

$$\log N = A_1 + A_2 (S)$$

$$A_1 = \frac{\sum \log N \sum (S^2) - \sum S \sum (S \log N)}{n \sum (S^2) - (\sum S)^2}$$

$$A_2 = \frac{n \sum (S \log N) - (\sum S)(\sum \log N)}{n \sum (S^2) - (\sum S)^2}$$

The results of the tensile testing for AM355 are presented in tabular format in Table 7.

Table 7. Laminate Mechanical Test Data

Specimen Designation	Cross-Sectional Area	UTS (KSI)	0.2% Yield Stress (KSI)	% Elongation
LCAR	0.0096	240	194	15.6
LCBL	0.0096	242	227	17.9
TR 4	0.0093	250	189	19.6
TR 20	0.0093	246	185	17.4
TL 4	0.0093	250	179	17.0
TL 20	0.0093	251	198	19.7
6800 R 10	0.0092	253	249	15.4
6800 R 11	0.0092	256	250	15.5
KSD-AL	0.00927	251.3	219.8	24.1
KSD-BL	0.00927	249.7	210.4	24.6
KSD-DL	0.0093	254.8	212.1	23.6

## 7. DISCUSSION

It can be clearly seen from the optical and electron microscopy results that the surface intergranular condition has an effect on the initiation and progression of a fatigue crack front. The intergranular network of attack on the surface of the material has been measured to be approximately 100–250  $\mu\text{in}$  deep, varying upon the location measured and the coil of material from which the specimens were acquired. The intergranular attack is present on both sides of the material and constitutes approximately 2.5% of the total cross-sectional area (using 175  $\mu\text{in}$  as the average depth of the intergranular surface attack and the fact that the material is only approximately 0.014 in thick). The significance of 2.5% of the cross-sectional area being attacked can be clearly seen in the micrographs and in the fatigue data. The intergranular attack lowers the fatigue life of the material simply because a fatigue crack front can easily follow the intergranular network of attack near the surface, and less energy is needed to propagate the crack. The specimens with no surface intergranular attack failed from either edge scratches or surface pits from service. The specimens with a surface intergranular attack failed mostly from edge scratches. However, specimen "low-cost" AR failed from the surface intergranular attack. These specimens had the most severe intergranular attack. Although this merits further investigation, it must be accepted that severe intergranular attack of the surface of the laminates can initiate fatigue failures. The crack obviously progressed along the intergranular network near

the surface edges of the specimens that exhibited surface intergranular attack. This mode was not evident on the specimens that did not contain significant surface intergranular attack. It would be expected that having an intergranular network (from the intergranular attack) on the surface of the laminates would lower the fatigue life of the material. This was demonstrated in the graphical presentation of the fatigue data. It can clearly be seen in all three fits of the data that the "Trial" and "KSD" specimens have lower overall and projected fatigue lives. It would be interesting to further study the material labeled "low cost," since it would be expected to have the lowest fatigue life because of the severity of its intergranular attack of the surface. The tensile data all fell within the normal values for the material. It appears that the surface intergranular condition does not have a significant effect on the tensile properties of the material.

## 8. CONCLUSION

The S/N curves generated as a result of fatigue data produced from specimens of AM355 material having intergranular surface attack are lower (2–10-ksi cyclic stress amplitude for similar cycles) than those for similar specimens without this surface attack.

## 9. RECOMMENDATIONS

The results of this work demonstrate a reduction in fatigue resistance for specimens having an intergranular network of attack of the surface of the material. The effect of the intergranular attack on the fatigue properties needs to be quantified by using material from the same coil (i.e., the same heat treat and surface conditions). Therefore, the material could be tested with the intergranular attack present and with it removed, while all other variables remain constant. Data from a study of this nature could be used to project the fatigue life of material now in service.



Figure 1. SEM fractograph of 11L from SP #7888 showing an edge origin. Mag. 250x.

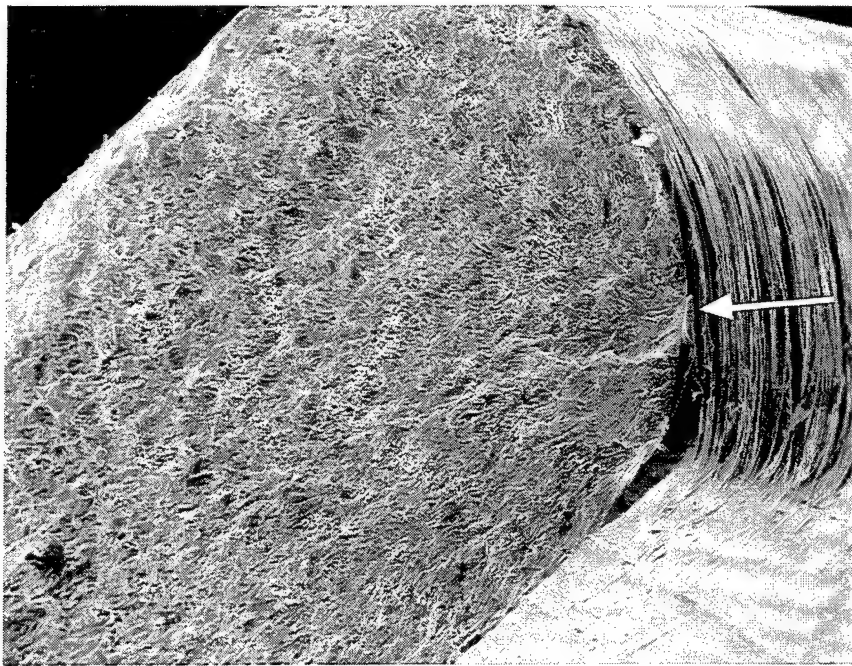


Figure 2. SEM fractograph of 11L from SP #7888 showing edge scratches. Mag. 250x.

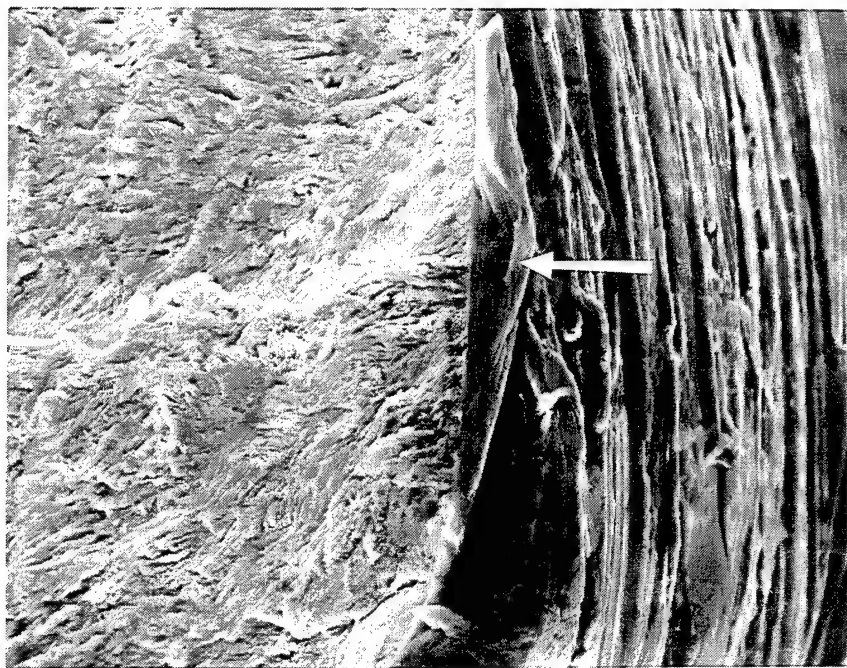


Figure 3. SEM fractograph of SP #7888 11L showing the scratch root origin. Mag. 1000 $\times$ .

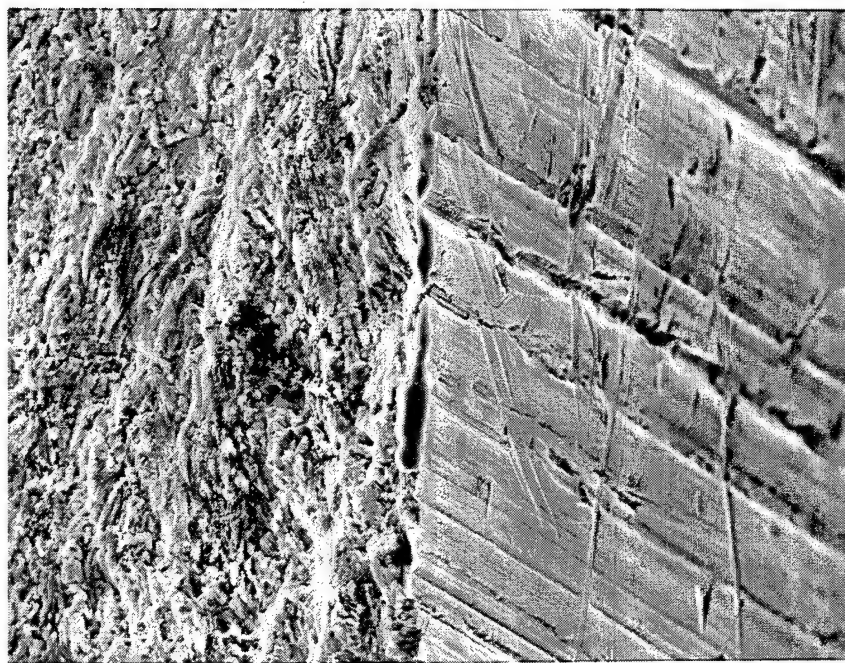


Figure 4. SEM fractograph of SP #7888 11L showing lack of intergranular edge. Mag. 750 $\times$ .

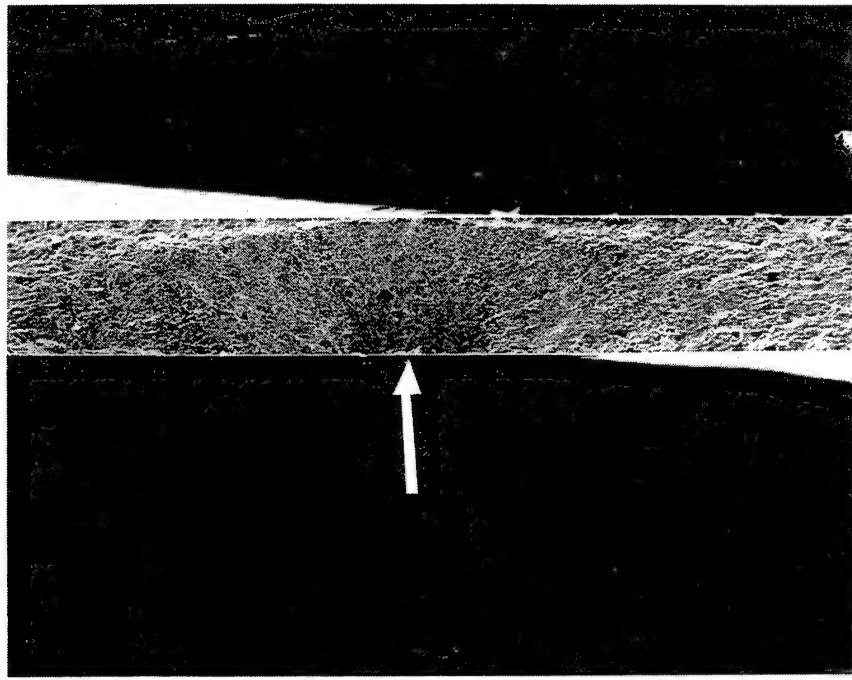


Figure 5. SEM fractograph of 10L from SP #6800 showing thumbnail origin. Mag. 50x.

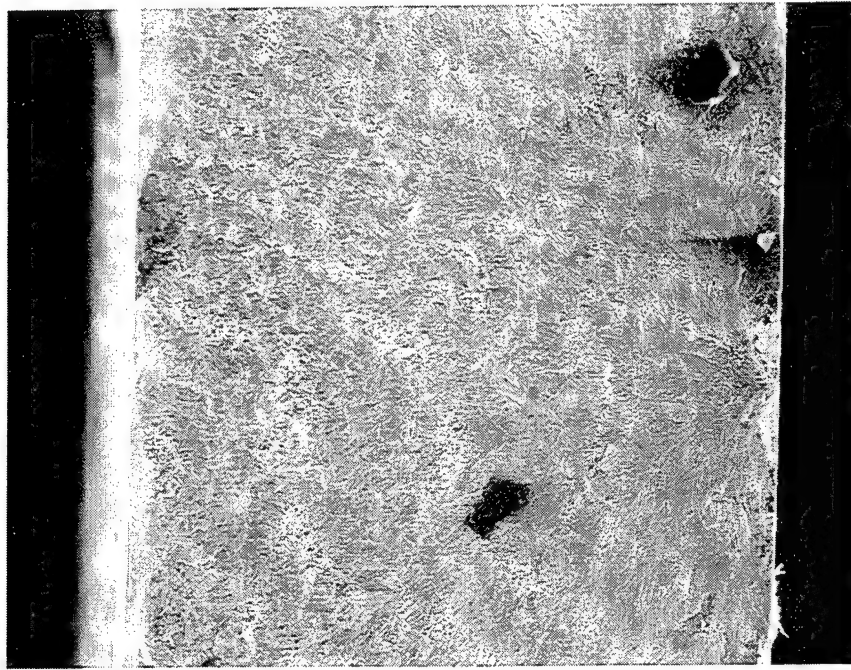


Figure 6. SEM fractograph of SP #6800 10L showing the origin. Mag. 250x.

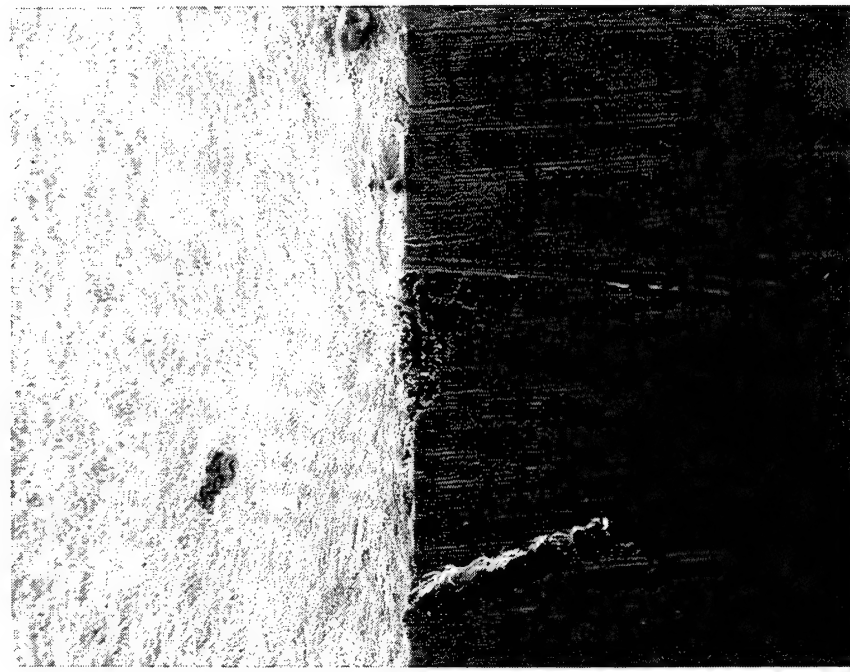


Figure 7. SEM fractograph of SP #6800 10L showing the surface pit origin. Mag. 250 $\times$ .

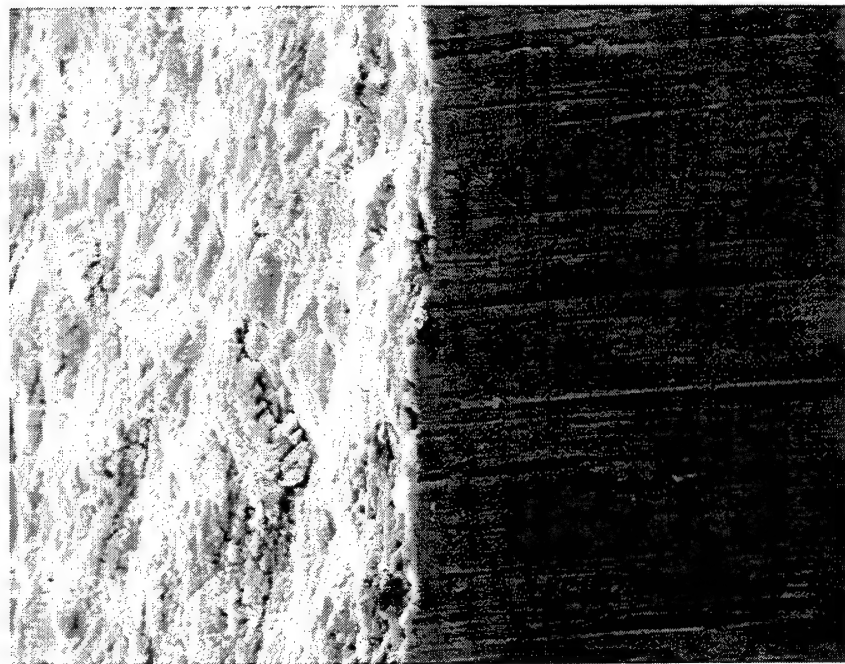


Figure 8. SEM fractograph of SP #6800 10L showing lack of intergranular edge. Mag. 1000 $\times$ .



Figure 9. SEM fractograph of Trial R12 showing an edge origin. Mag. 250 $\times$ .

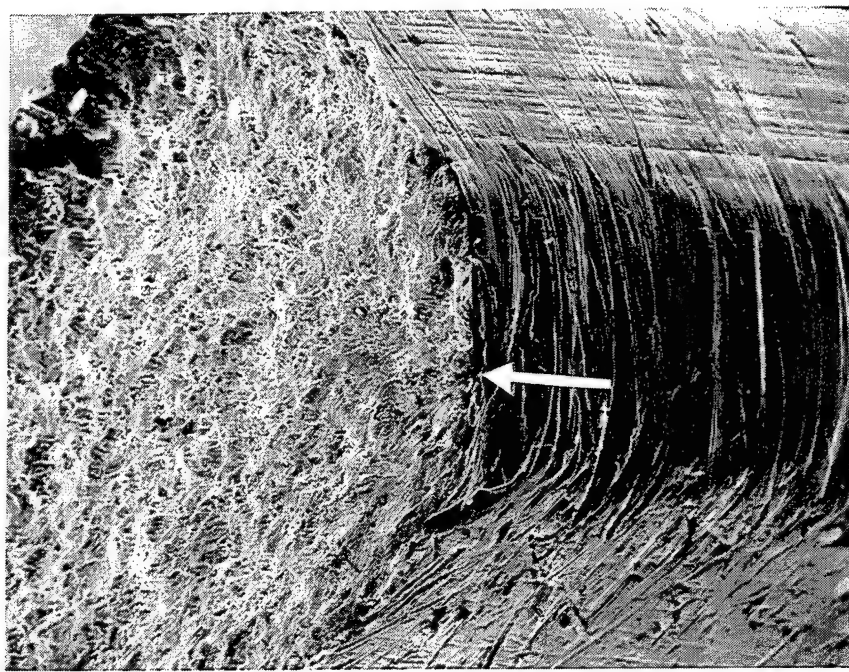


Figure 10. SEM fractograph of Trial R12 showing edge scratches. Mag. 250 $\times$ .

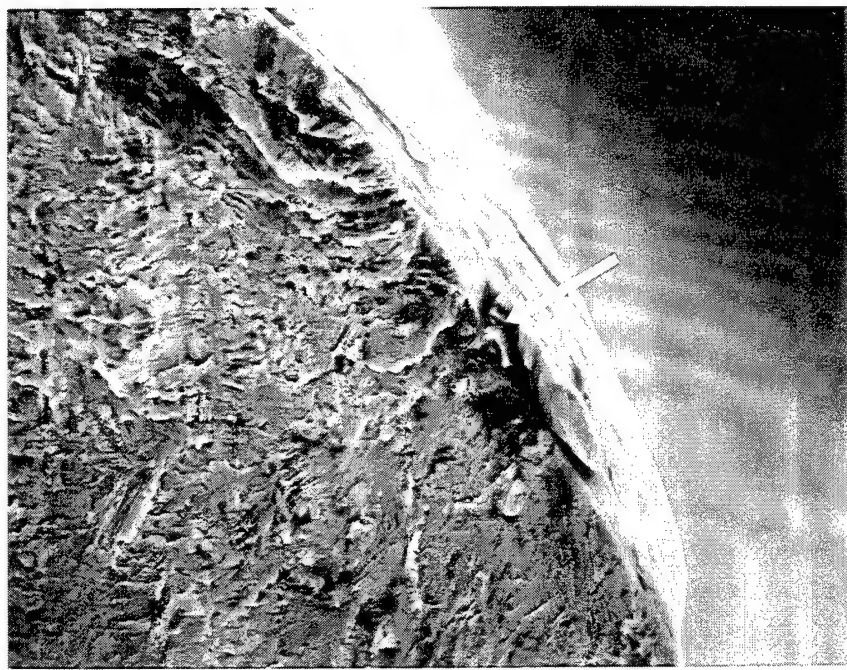


Figure 11. SEM fractograph of Trial R12 showing an edge scratch origin. Mag. 1000 $\times$ .

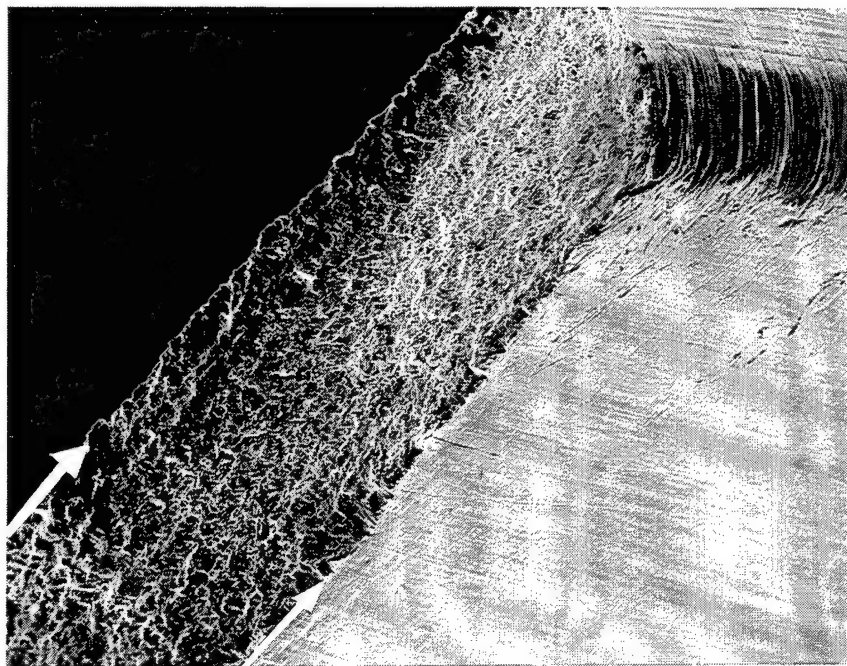


Figure 12. SEM fractograph of Trial R12 showing fatigue by edge intergranular. Mag. 100 $\times$ .

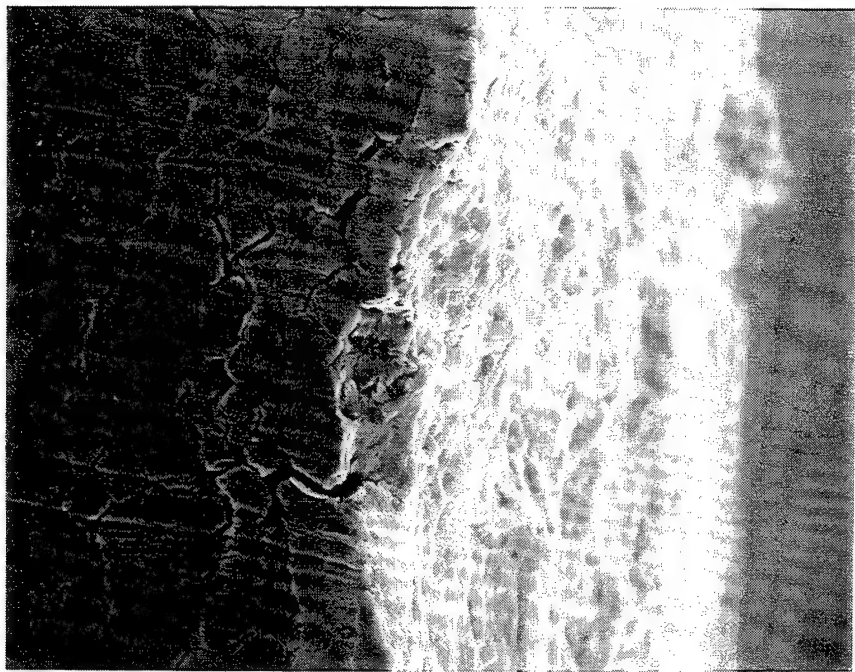


Figure 13. SEM fractograph of Trial R12 showing removed grains on edge. Mag. 750 $\times$ .

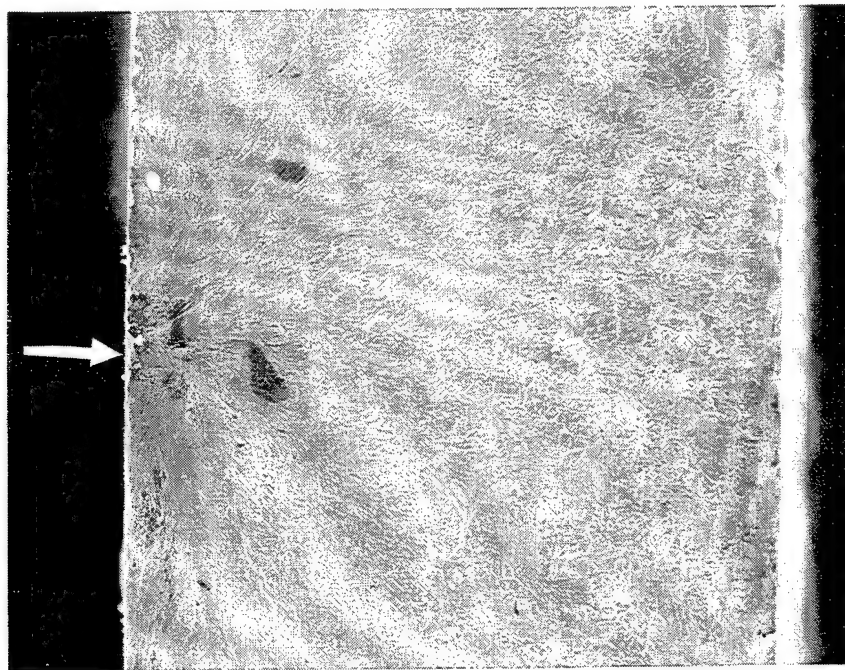


Figure 14. SEM fractograph of low-cost AR showing surface failure origin. Mag. 250 $\times$ .

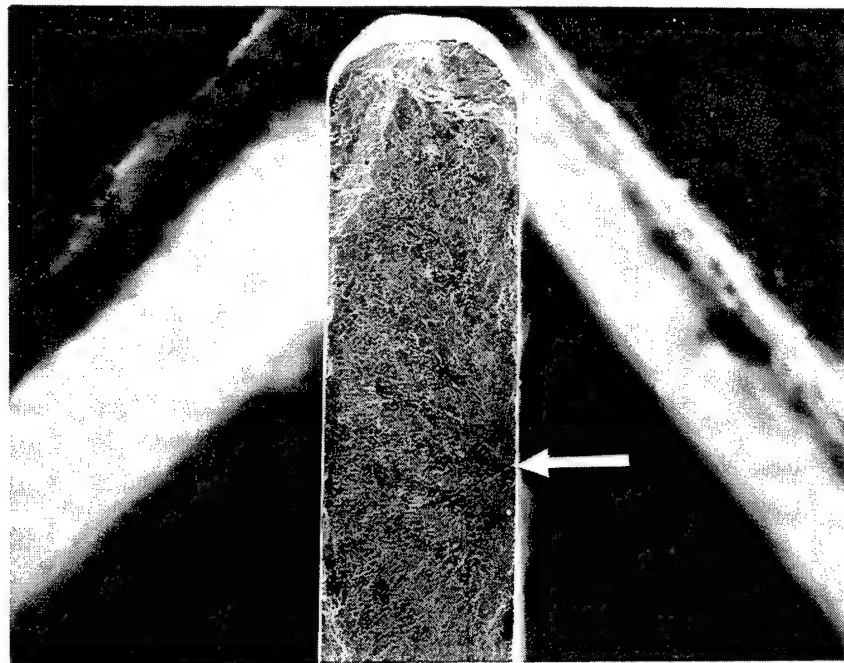


Figure 15. SEM fractograph of low-cost AR showing location of surface origin. Mag. 100 $\times$ .

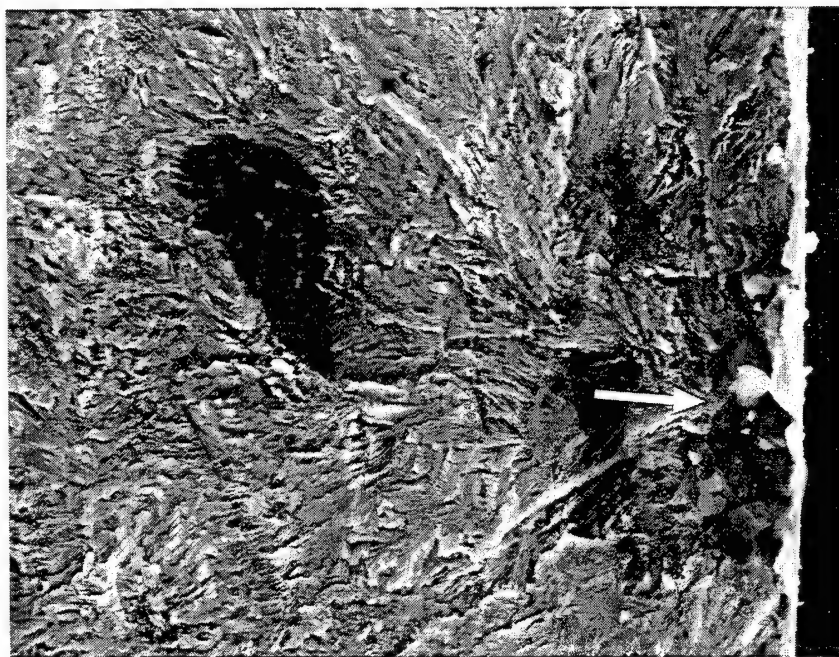


Figure 16. SEM fractograph of low-cost AR showing intergranular at origin. Mag. 1000 $\times$ .



Figure 17. SEM fractograph of low-cost AR intergranular attack near the origin. Mag. 500 $\times$ .

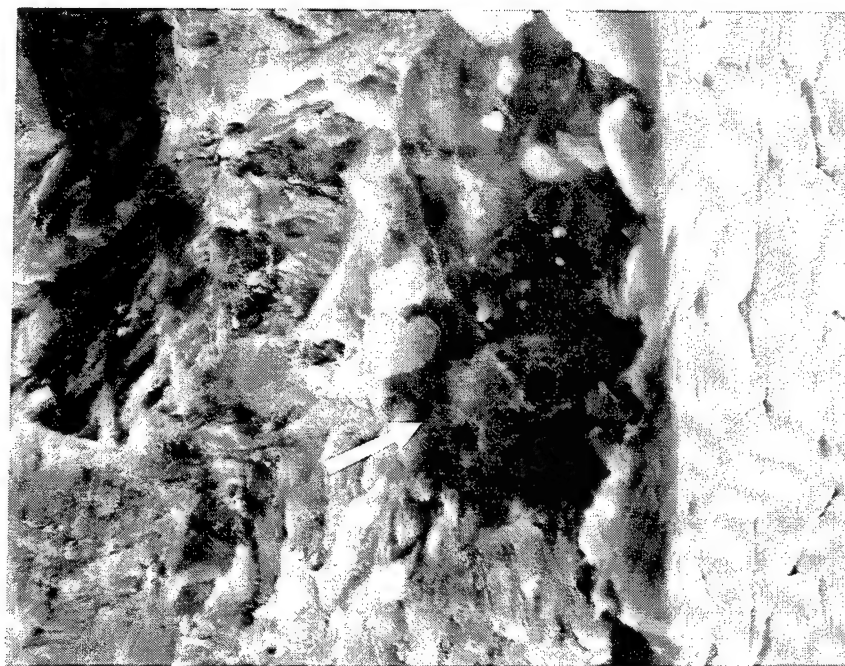


Figure 18. SEM fractograph of low-cost AR intergranular morphology at origin. Mag. 3000 $\times$ .

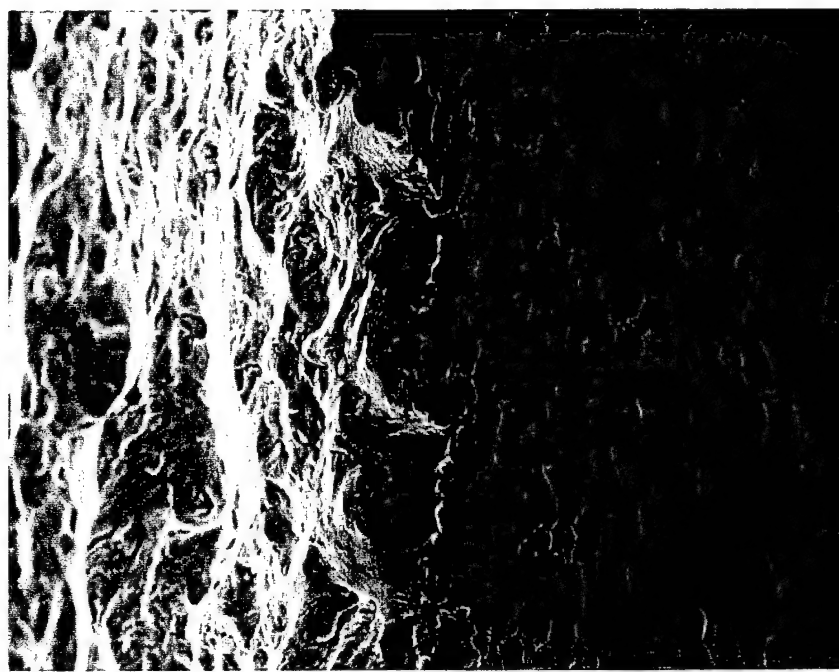


Figure 19. SEM fractograph of low-cost AR removed edge grains and secondary cracking origin. Mag. 500 $\times$ .

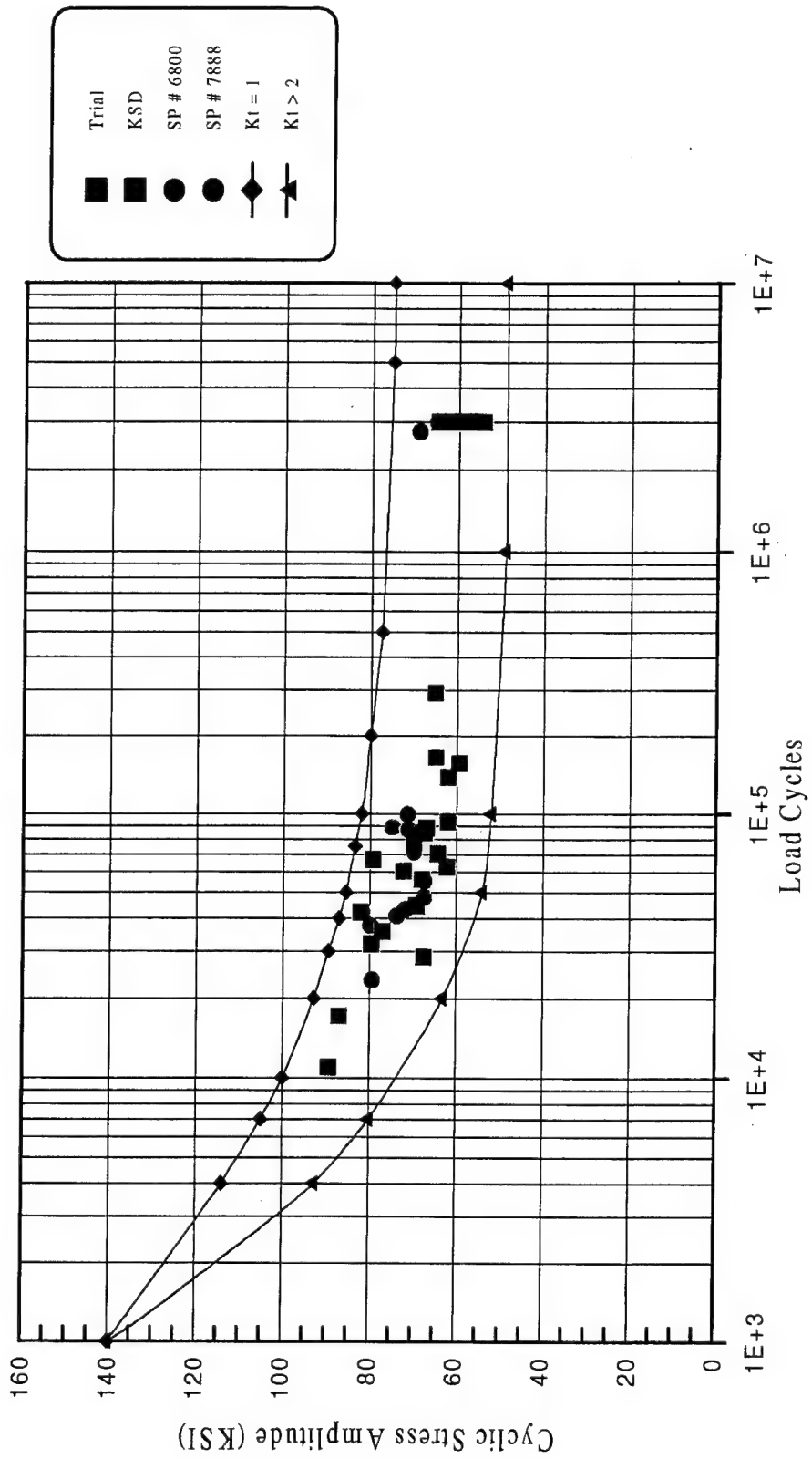


Figure 20. AM355 axial fatigue test - S-N curve:  $K_t = 1$ ;  $T = 0.014$ ;  $G = 0.660$ ;  $R = 0.05$ .

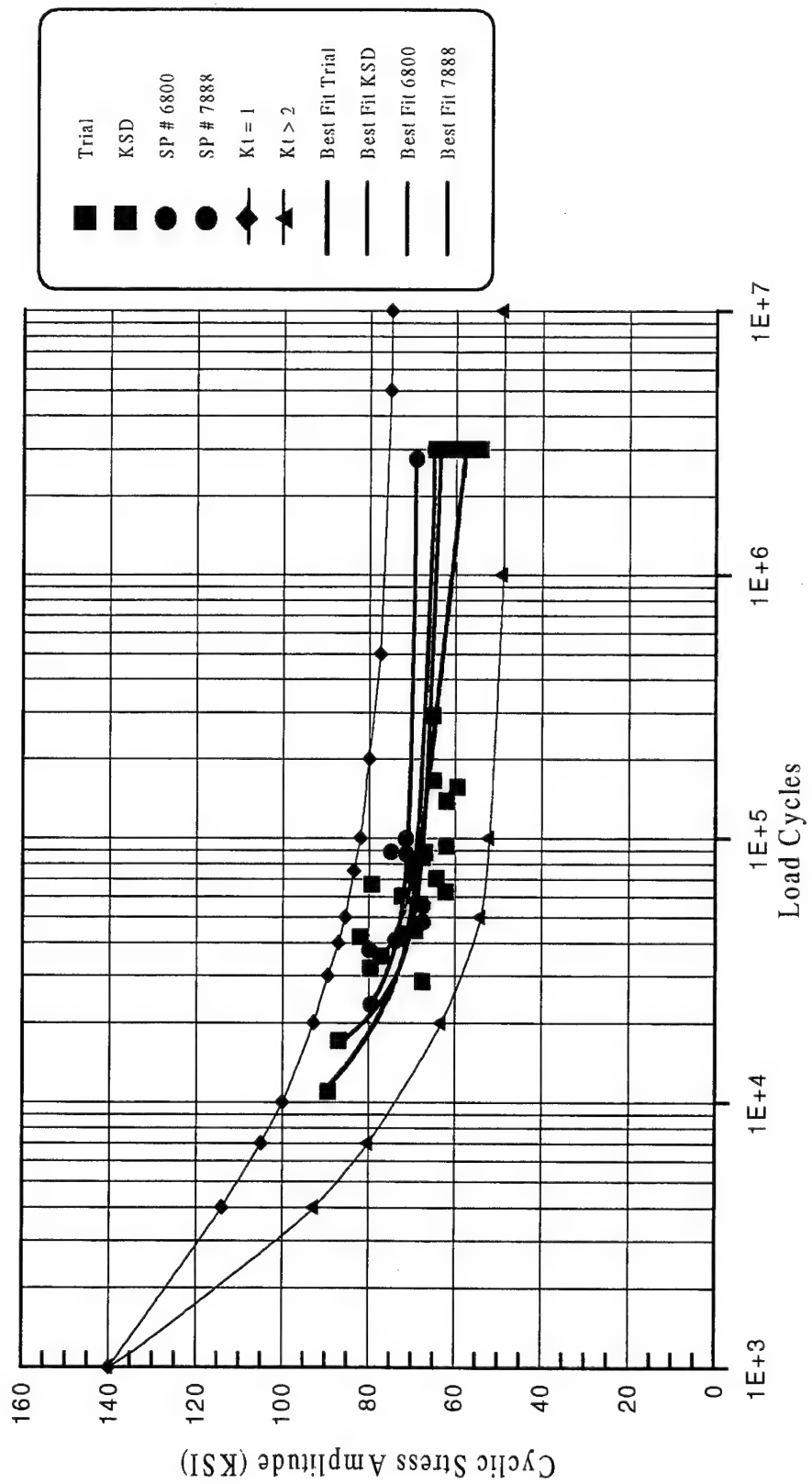


Figure 21. AM355 axial fatigue test - S-N curve;  $Kt = 1$ ;  $T = 0.014$ ;  $G = 0.660$ ;  $R = 0.05$ ; best-fit curves.

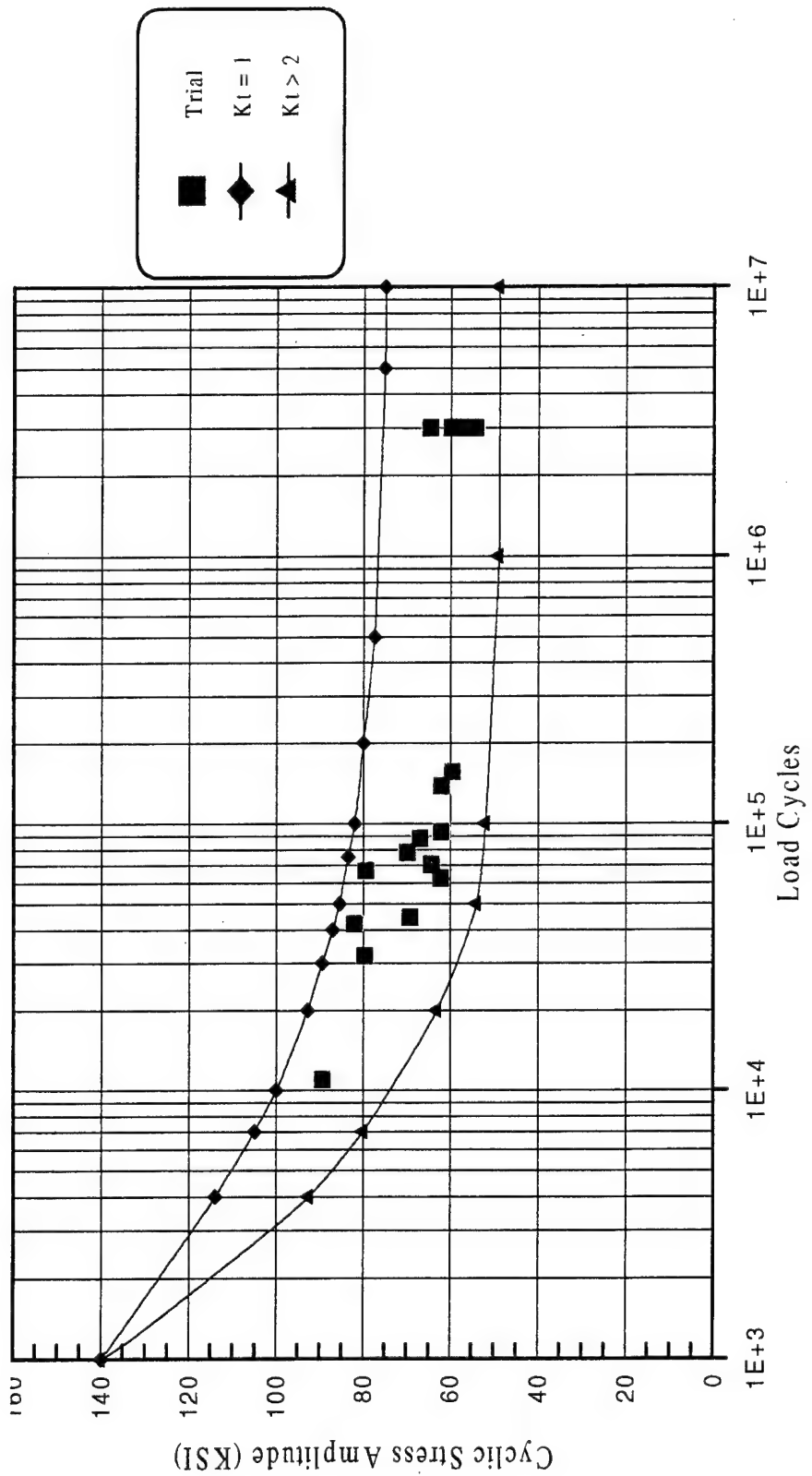


Figure 22. AM355 axial fatigue test - S-N curve:  $K_I = 1$ ;  $T = 0.014$ ;  $G = 0.660$ ;  $R = 0.05$ ; trial.

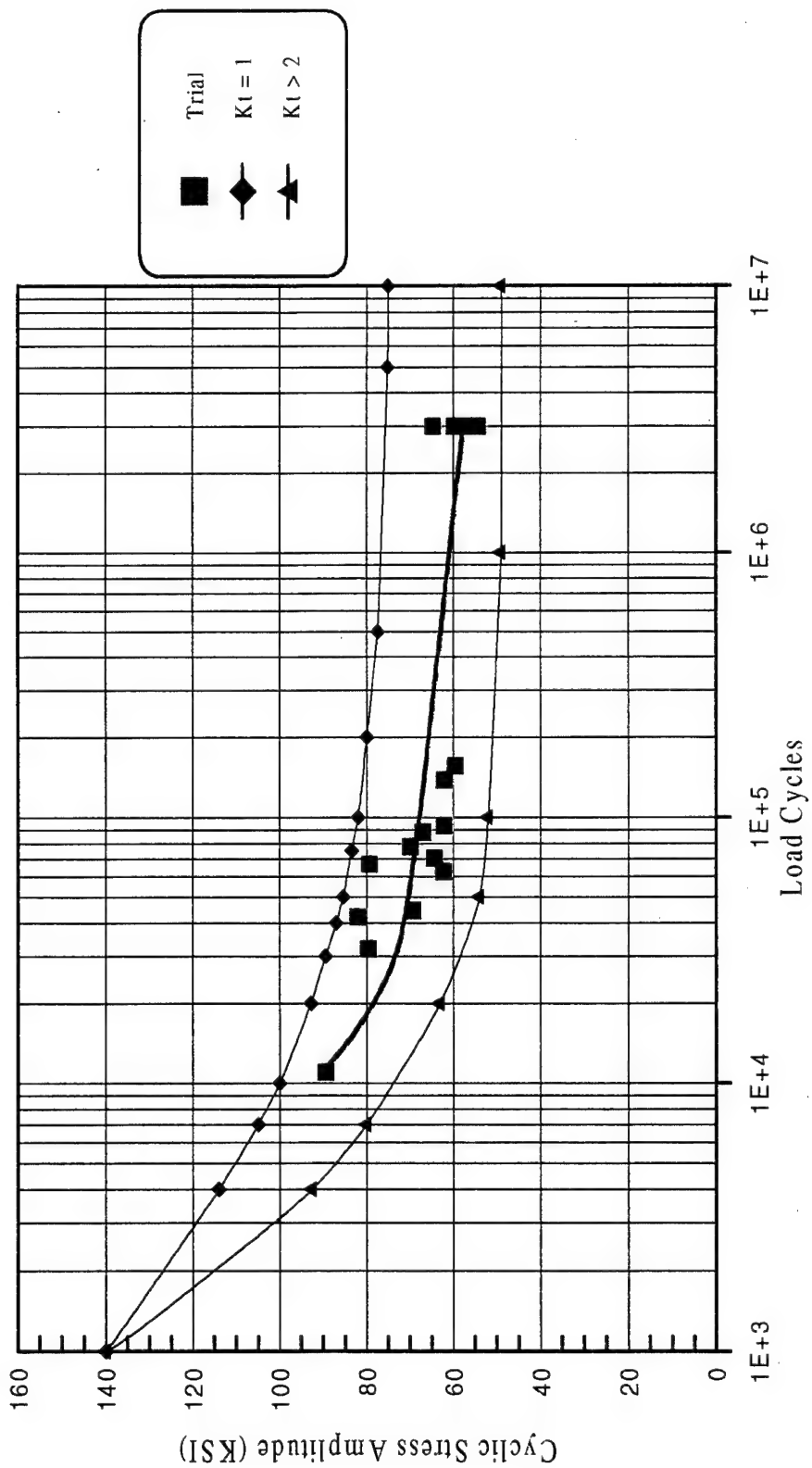


Figure 23. AM355 axial fatigue test - S-N curve;  $K_t = 1$ ;  $T = 0.014$ ;  $G = 0.660$ ;  $R = 0.05$ ; trial best fit.

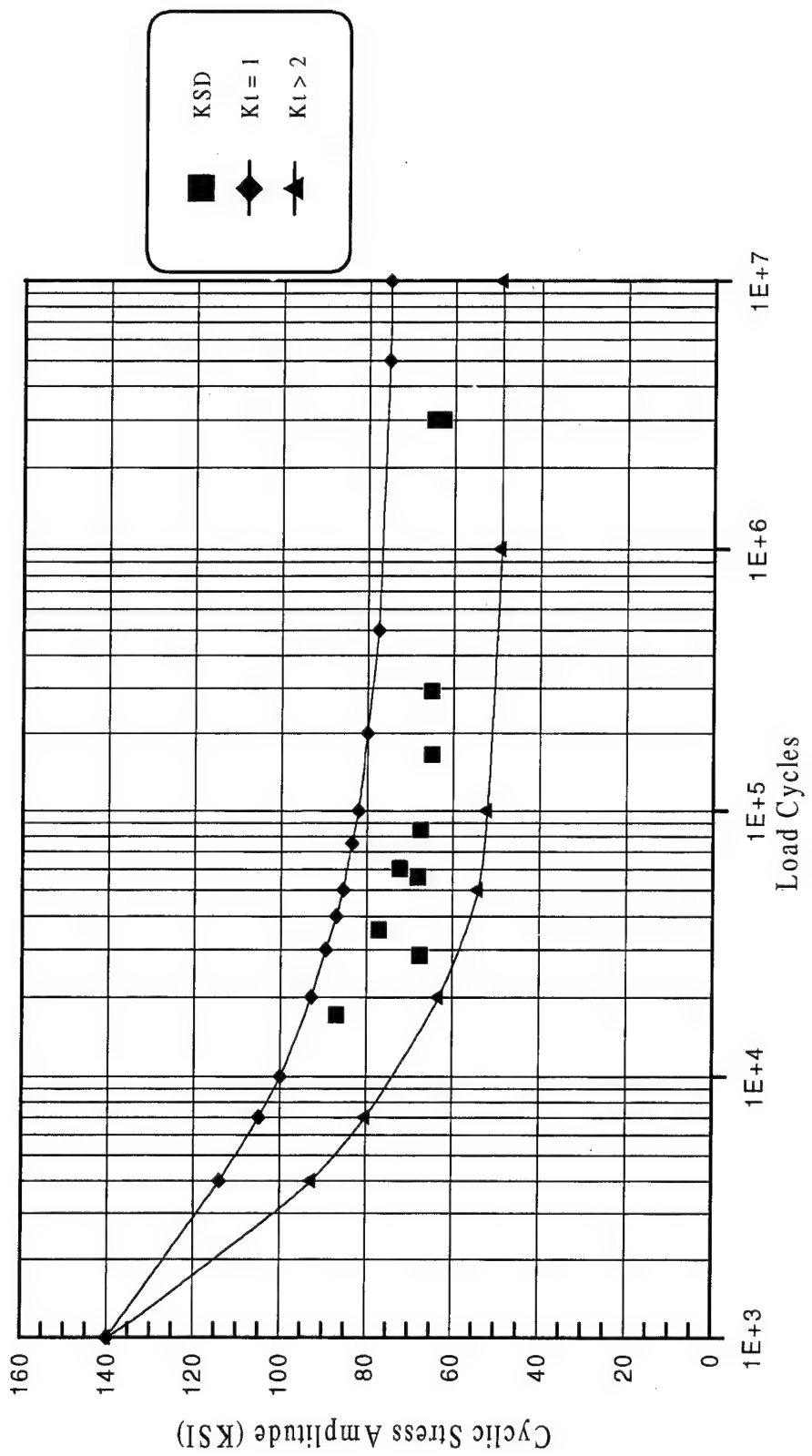


Figure 24. AM355 axial fatigue test - S-N curve;  $K_t = 1$ ;  $T = 0.014$ ;  $G = 0.660$ ;  $R = 0.05$ ; KSD.

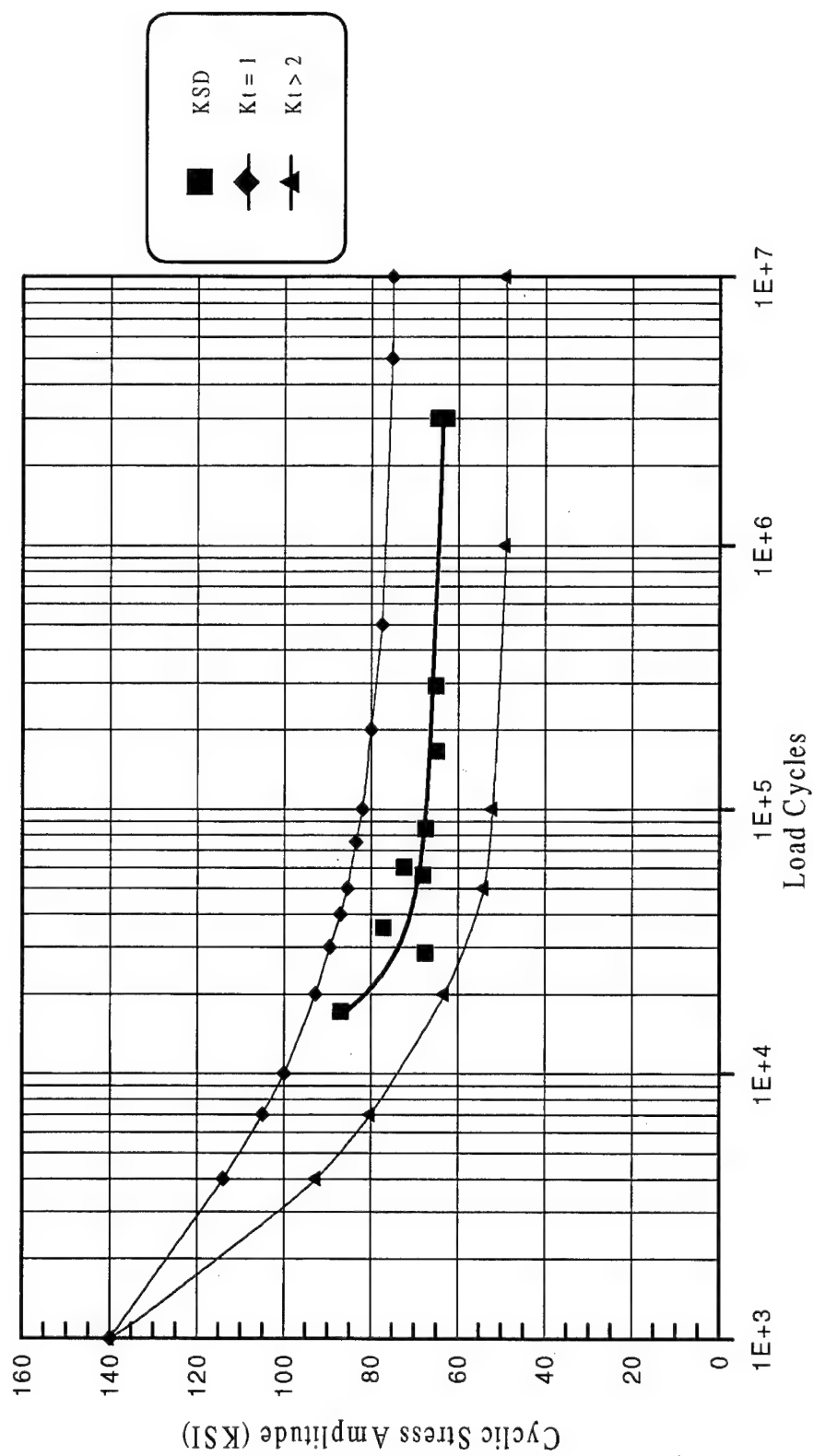


Figure 25. AM355 axial fatigue test - S-N curve;  $K_t = 1$ ;  $T = 0.014$ ;  $G = 0.660$ ;  $R = 0.05$ ; KSD best fit.

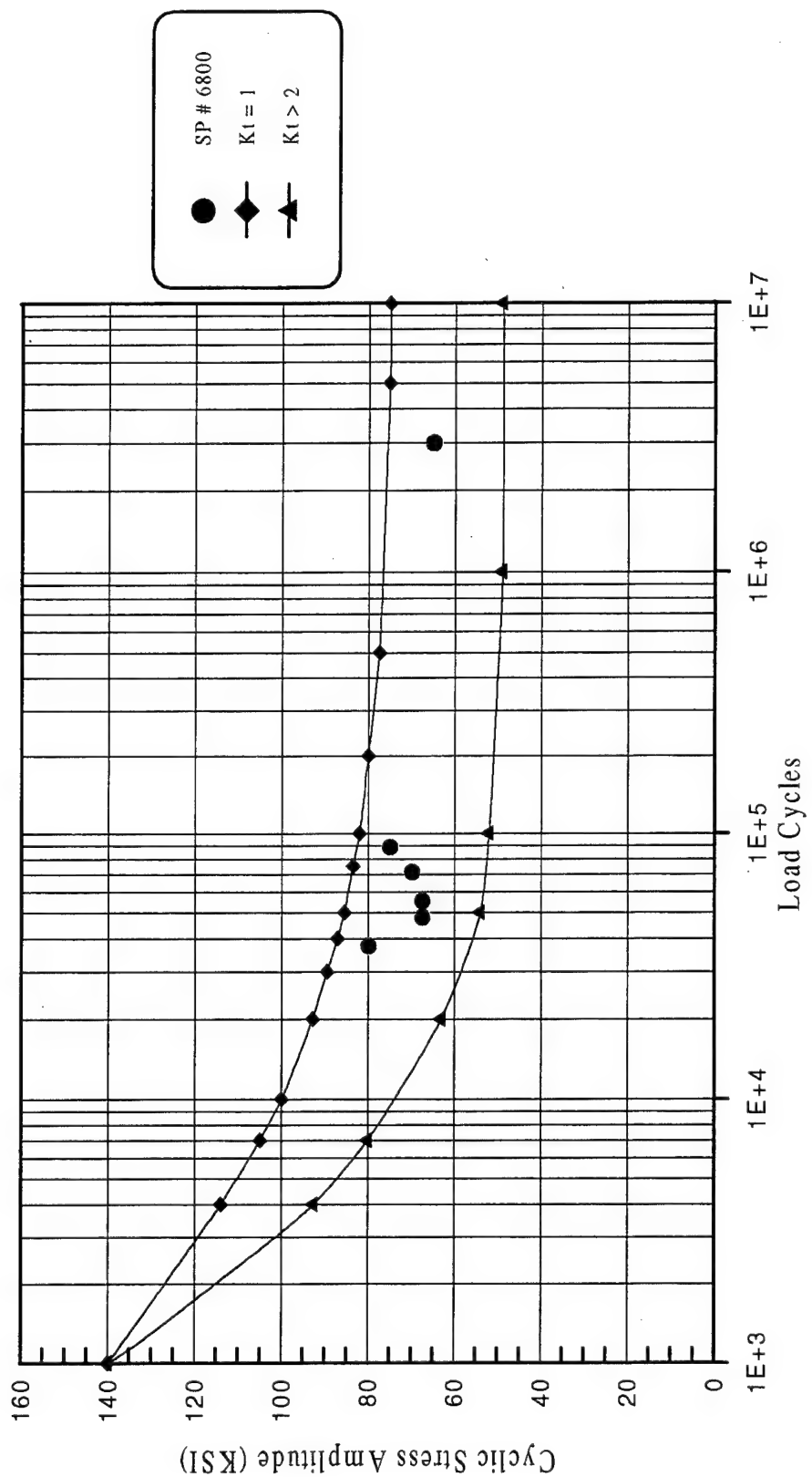


Figure 26. AM355 axial fatigue test - S-N curve:  $K_t = 1$ ;  $T = 0.014$ ;  $G = 0.660$ ;  $R = 0.05$ ; SP #6800.

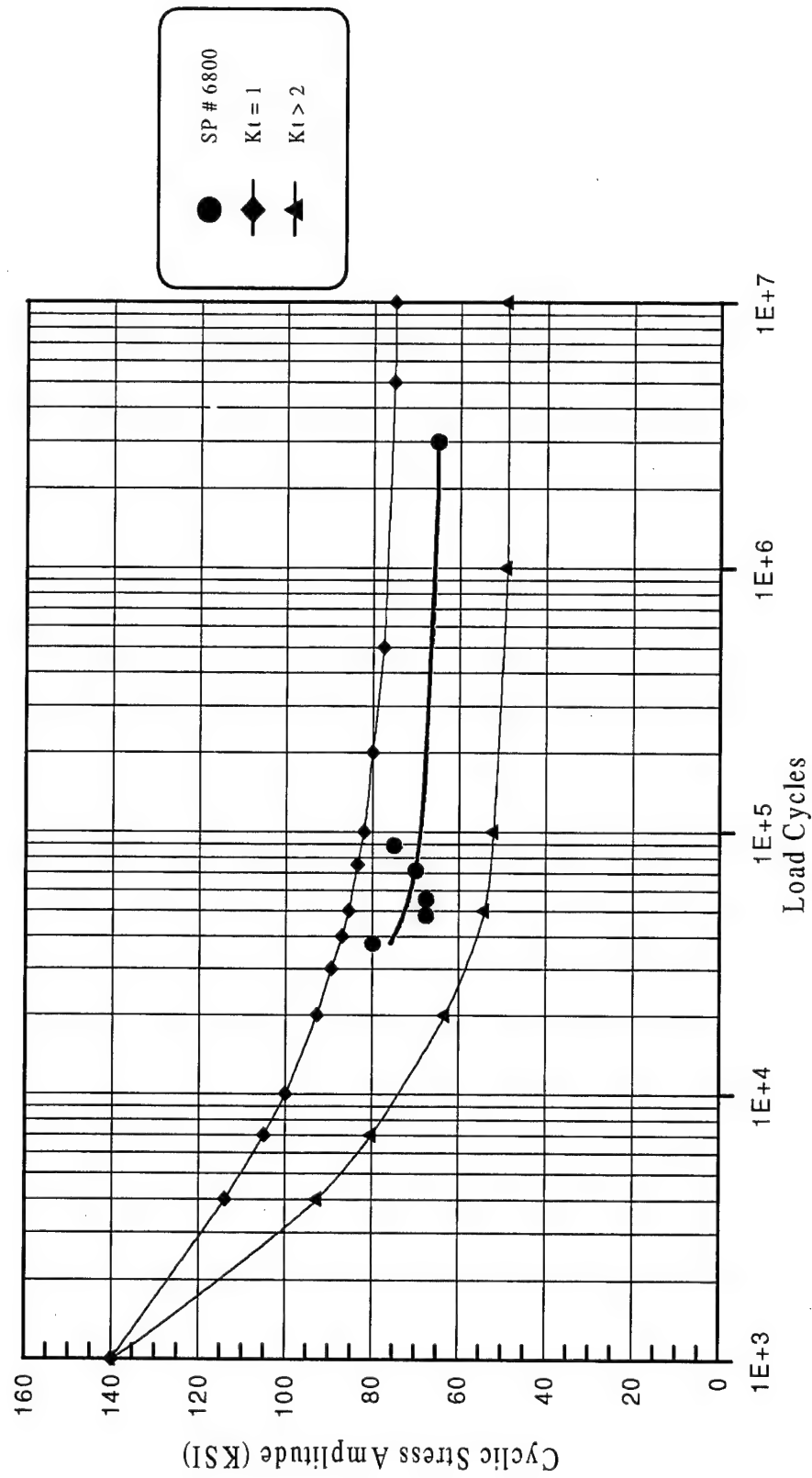


Figure 27. AM355 axial fatigue test - S-N curve:  $K_t = 1$ ;  $T = 0.014$ ;  $G = 0.660$ ;  $R = 0.05$ ; SP #6800 best fit.

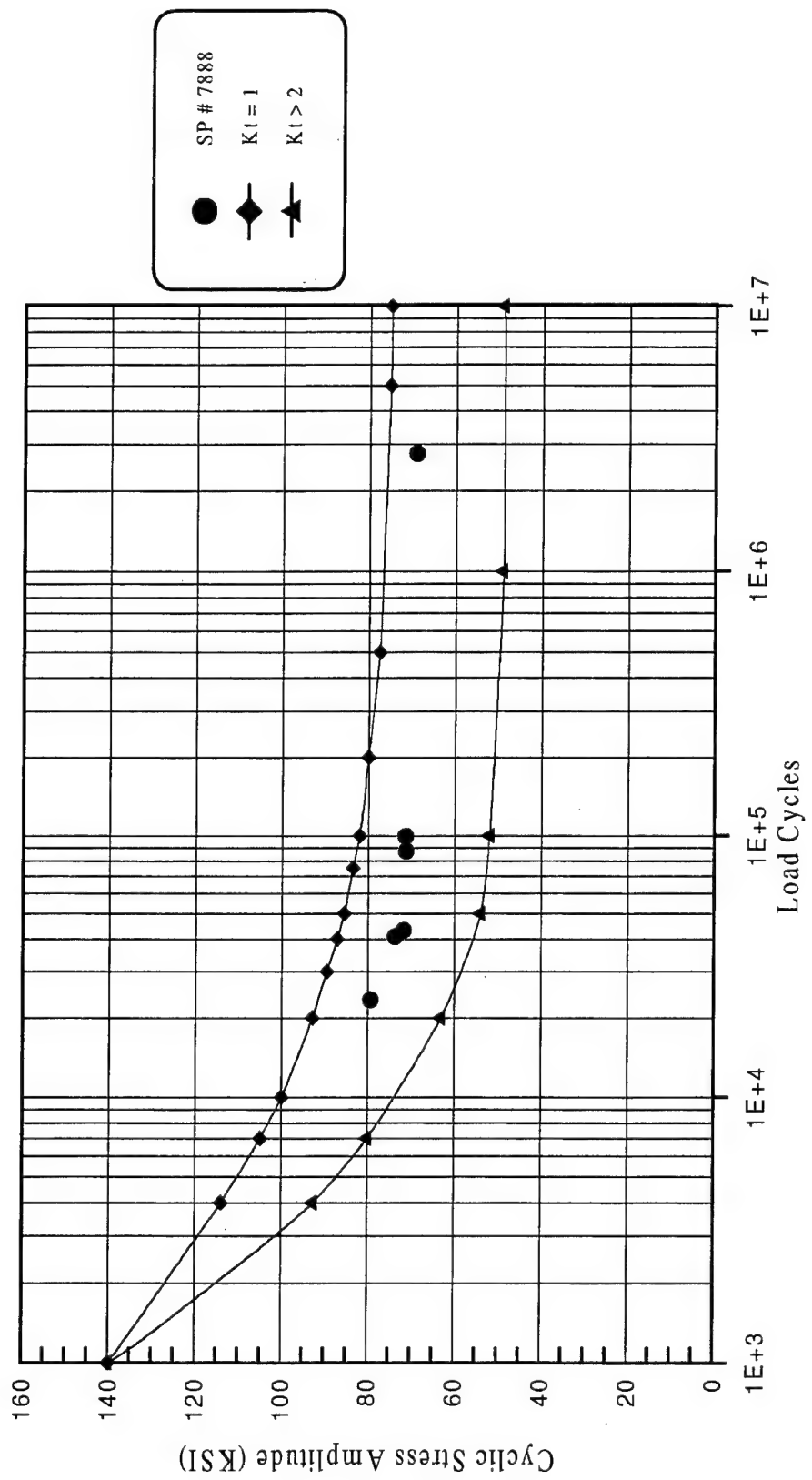


Figure 28. AM355 axial fatigue test - S-N curve:  $K_t = 1$ ;  $T = 0.014$ ;  $G = 0.660$ ;  $R = 0.05$ ; SP #7888.

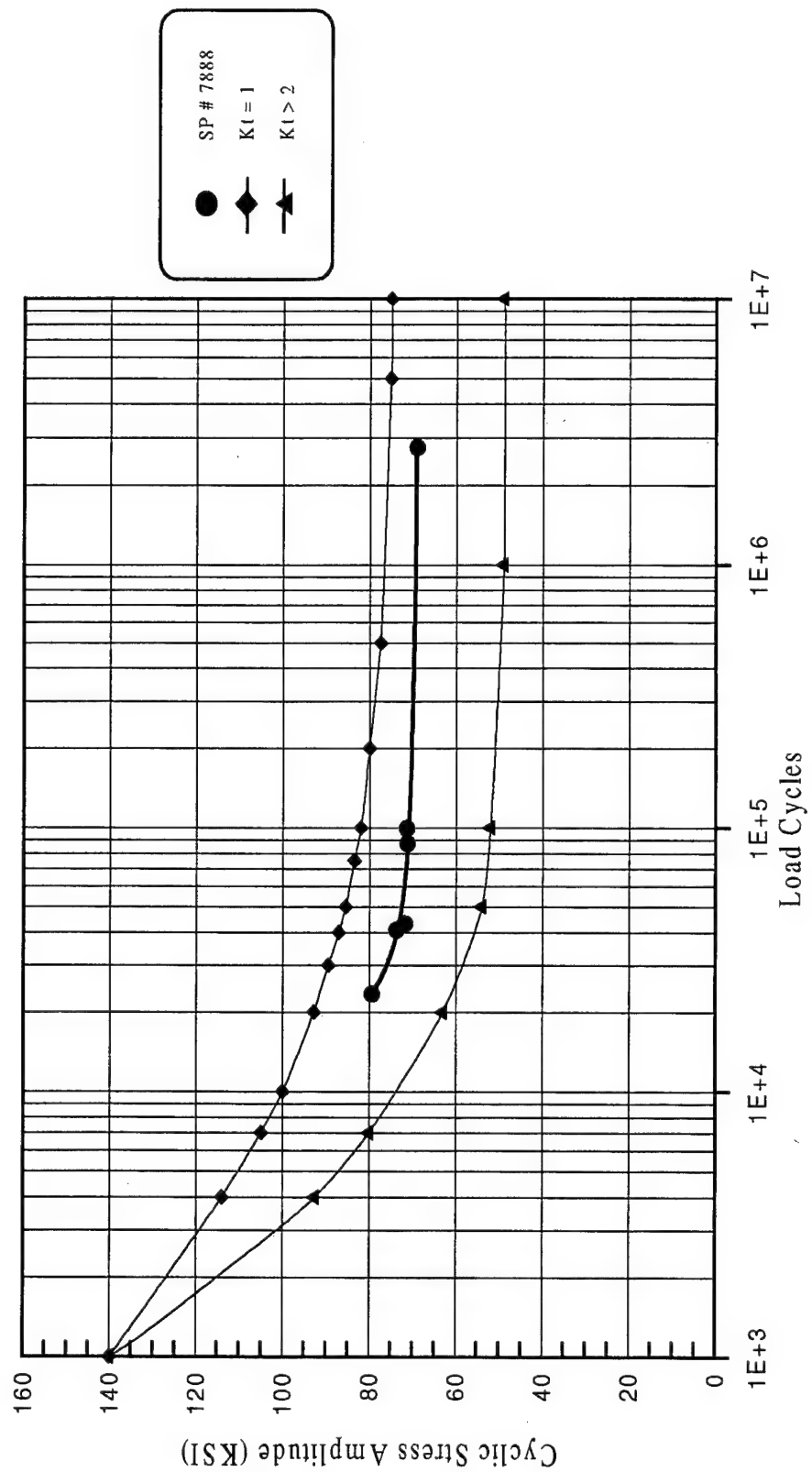


Figure 29. AM355 axial fatigue test - S-N curve;  $Kt = 1$ ;  $\Gamma = 0.014$ ;  $G = 0.660$ ;  $R = 0.05$ ; SP #7888 best fit.

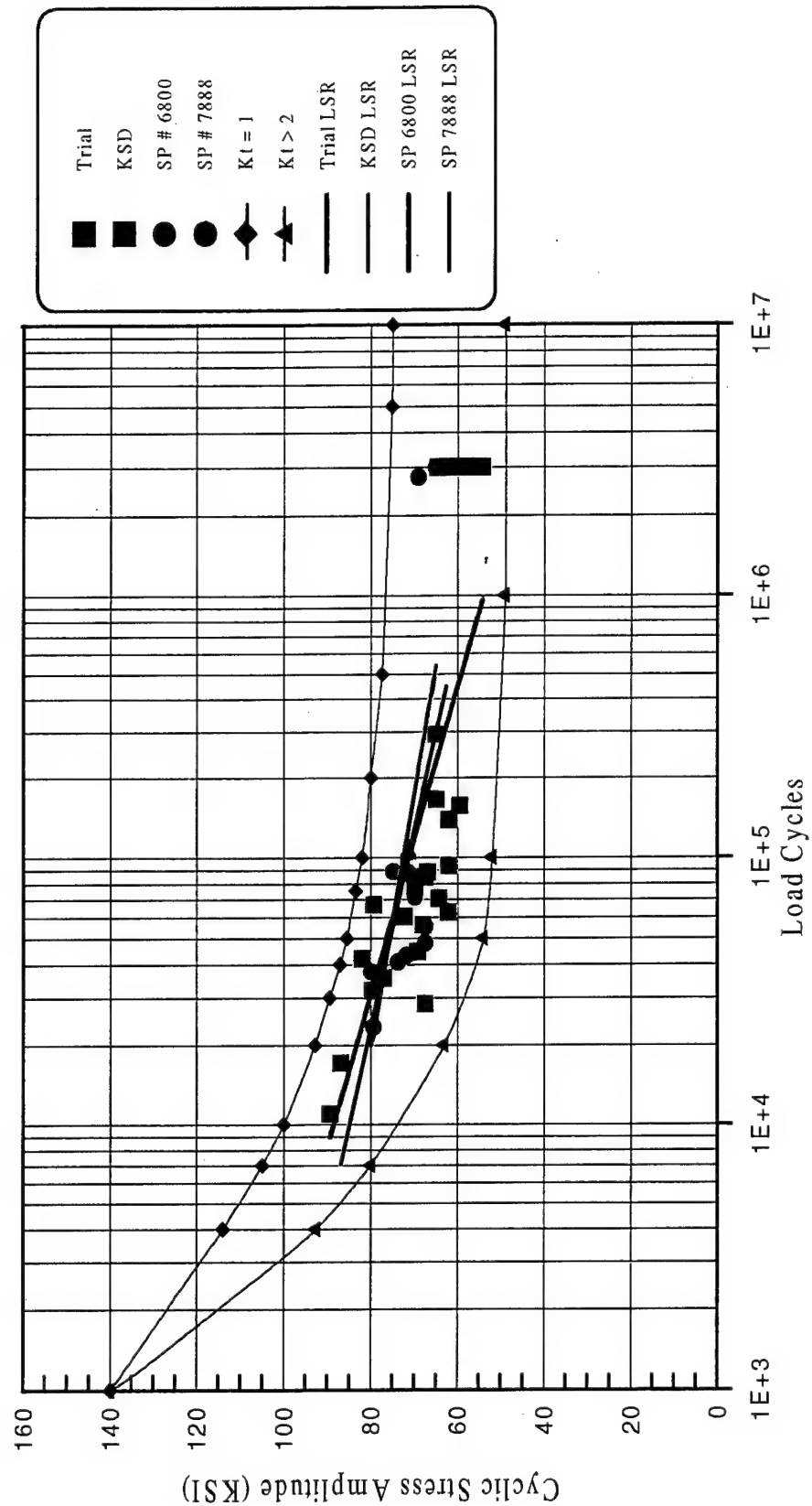


Figure 30. AM355 axial fatigue test - S-N curve;  $Kt = 1$ ;  $\Gamma = 0.014$ ;  $G = 0.660$ ;  $R = 0.05$ ; least-squares regression fit.

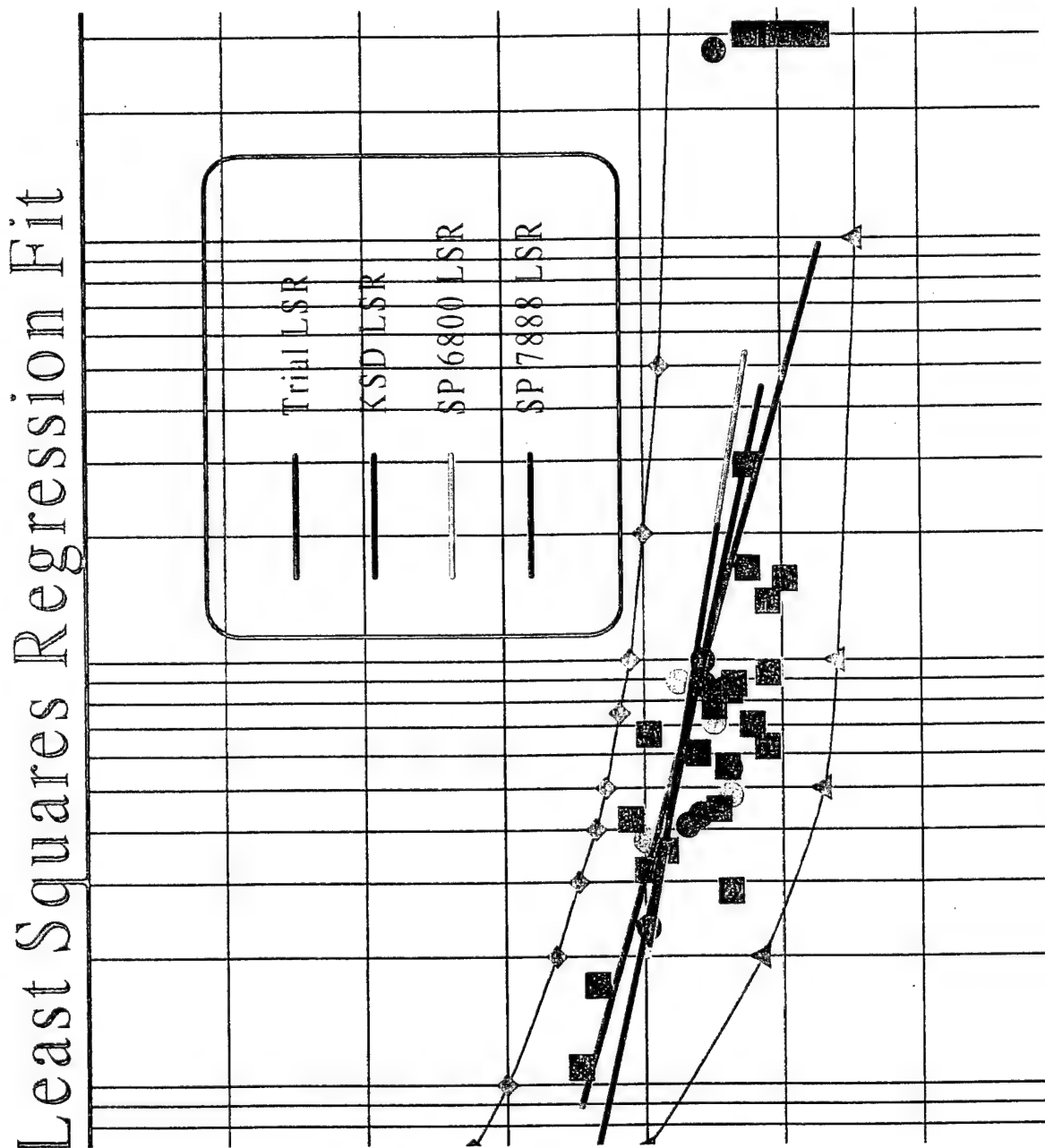


Figure 31. Least-squares regression fit.

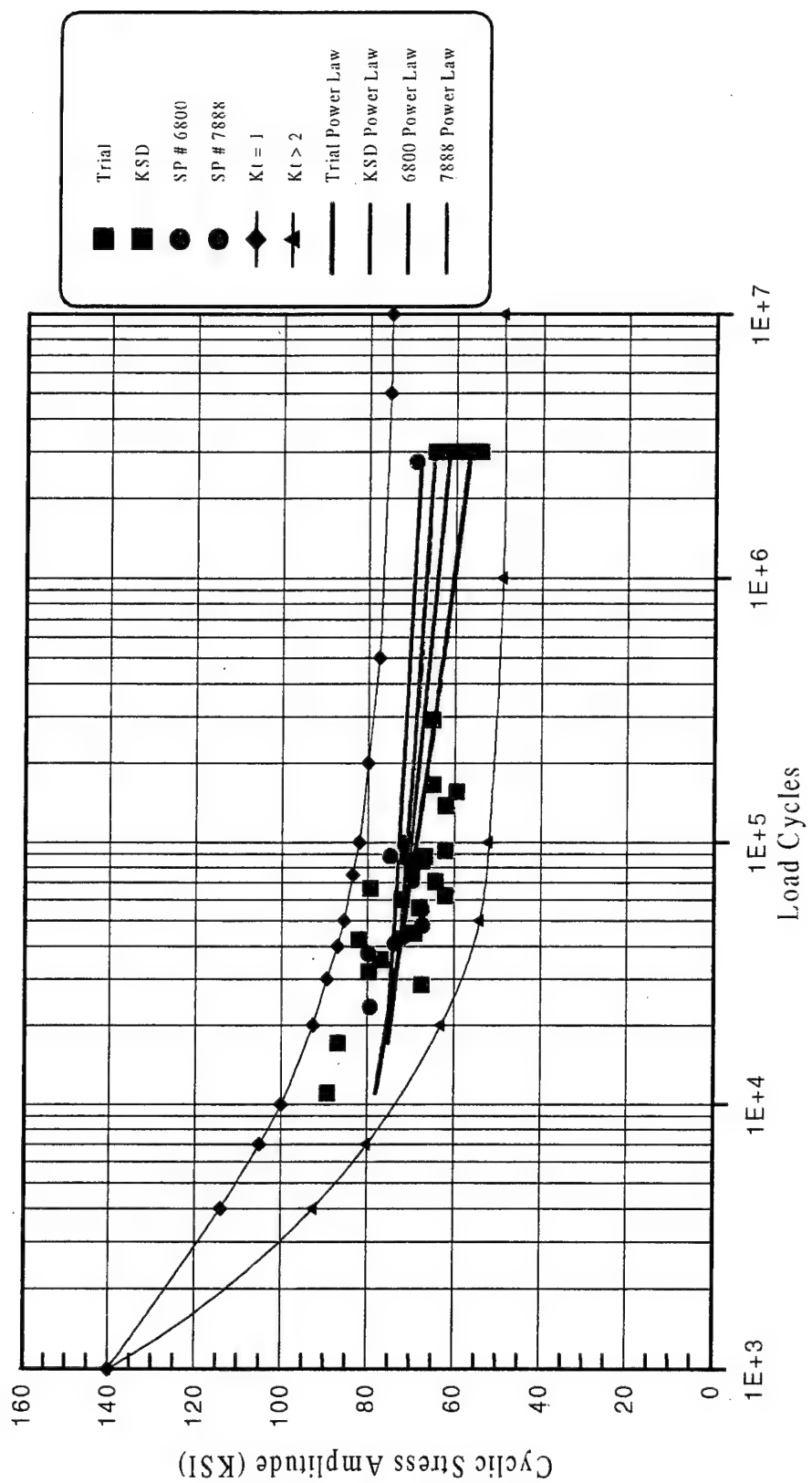


Figure 32. AM355 axial fatigue test - S-N curve;  $Kt = 1$ ;  $T = 0.014$ ;  $G = 0.660$ ;  $R = 0.05$ ; power law fit.

## Power Law Fit

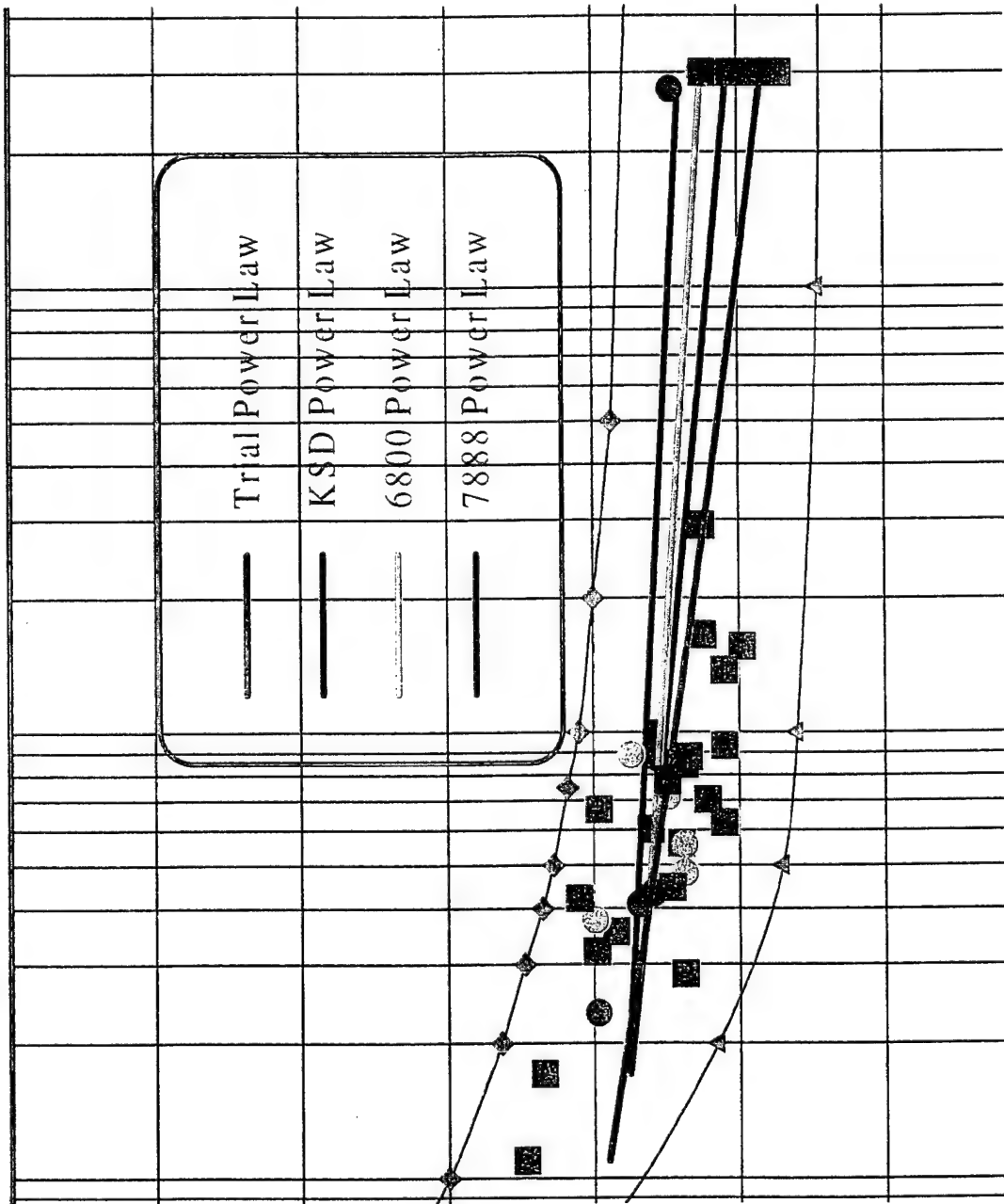


Figure 33. Power law fit.

INTENTIONALLY LEFT BLANK.

<u>NO. OF COPIES</u>	<u>ORGANIZATION</u>
2	DEFENSE TECHNICAL INFO CTR ATTN DTIC DDA 8725 JOHN J KINGMAN RD STE 0944 FT BELVOIR VA 22060-6218
1	DIRECTOR US ARMY RESEARCH LAB ATTN AMSRL CS AL TP 2800 POWDER MILL RD ADELPHI MD 20783-1145
1	DIRECTOR US ARMY RESEARCH LAB ATTN AMSRL CS AL TA 2800 POWDER MILL RD ADELPHI MD 20783-1145
3	DIRECTOR US ARMY RESEARCH LAB ATTN AMSRL CI LL 2800 POWDER MILL RD ADELPHI MD 20783-1145

ABERDEEN PROVING GROUND

2 DIR USARL  
ATTN AMSRL CI LP (305)

NO. OF  
COPIES    ORGANIZATION

2      DIRECTOR  
US ARMY AVIATION &  
TROOP COMMAND  
ATTN AMSAT R EFM  
DR KIRIT BHANSALI  
4300 GOODFELLOW BLVD  
ST LOUIS MO 63120-1798

ABERDEEN PROVING GROUND

2      DIR USARL  
ATTN AMSRL MA CB  
S GRENDAHL  
V CHAMPAGNE

## USER EVALUATION SHEET/CHANGE OF ADDRESS

This Laboratory undertakes a continuing effort to improve the quality of the reports it publishes. Your comments/answers to the items/questions below will aid us in our efforts.

1. ARL Report Number/Author ARL-TR-1238 (Grendahl) Date of Report November 1996

2. Date Report Received \_\_\_\_\_

3. Does this report satisfy a need? (Comment on purpose, related project, or other area of interest for which the report will be used.)  
\_\_\_\_\_  
\_\_\_\_\_

4. Specifically, how is the report being used? (Information source, design data, procedure, source of ideas, etc.)  
\_\_\_\_\_  
\_\_\_\_\_

5. Has the information in this report led to any quantitative savings as far as man-hours or dollars saved, operating costs avoided, or efficiencies achieved, etc? If so, please elaborate.  
\_\_\_\_\_  
\_\_\_\_\_

6. General Comments. What do you think should be changed to improve future reports? (Indicate changes to organization, technical content, format, etc.)  
\_\_\_\_\_  
\_\_\_\_\_

CURRENT  
ADDRESS

Organization \_\_\_\_\_  
Name \_\_\_\_\_  
Street or P.O. Box No. \_\_\_\_\_  
City, State, Zip Code \_\_\_\_\_

7. If indicating a Change of Address or Address Correction, please provide the Current or Correct address above and the Old or Incorrect address below.

OLD  
ADDRESS

Organization \_\_\_\_\_  
Name \_\_\_\_\_  
Street or P.O. Box No. \_\_\_\_\_  
City, State, Zip Code \_\_\_\_\_

(Remove this sheet, fold as indicated, tape closed, and mail.)  
**(DO NOT STAPLE)**

DEPARTMENT OF THE ARMY

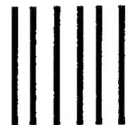
OFFICIAL BUSINESS

**BUSINESS REPLY MAIL**

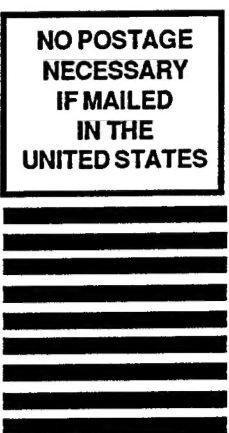
FIRST CLASS PERMIT NO 0001,APG,MD

POSTAGE WILL BE PAID BY ADDRESSEE

DIRECTOR  
U.S. ARMY RESEARCH LABORATORY  
ATTN: AMSRL-MA-C  
ABERDEEN PROVING GROUND, MD 21005-5069



NO POSTAGE  
NECESSARY  
IF MAILED  
IN THE  
UNITED STATES

A series of ten horizontal black bars of varying widths, used for postal processing.